

**Antragstellerin/Antragsteller:**

Lukas Prader

Akademischer Grad, Vorname/n, Nachname

Hocheggstraße 720, 6100 Seefeld in Tirol

Anschrift: Straße, PLZ und Ort

lukas.prader@tutanota.com, +43 650 6533276

E-Mail, Telefonnummer

Matrikelnummer:

12115058

Kennzeichnung des Studiums

UC 033 630

# Einreichung der Bachelorarbeit

(gem. § 80 Universitätsgesetz 2002 – UG)

**Titel der Bachelorarbeit:**

---

---

---

**Angaben zur Lehrveranstaltung** (im Rahmen welcher die Bachelorarbeit verfasst und positiv beurteilt worden ist):SE Biologisches Seminar: Ökologie

Titel der Lehrveranstaltung

743411

Lehrveranstaltungsnummer

4

Semester

Univ.-Prof. Mag. Dr. Gabriel Singer

Name der Lehrveranstaltungsleiterin / des Lehrveranstaltungsleiters

Ich erkläre hiermit an Eides statt durch meine eigenhändige Unterschrift, dass ich die vorliegende Arbeit selbstständig verfasst und keine anderen als die angegebenen Quellen und Hilfsmittel verwendet habe. Alle Stellen, die wörtlich oder inhaltlich den angegebenen Quellen entnommen wurden, sind als solche kenntlich gemacht.

Ich stimme einer Archivierung der Bachelorarbeit am Institut / an der Fakultät zu:

 Ja Nein

Datum

Unterschrift der/des Studierenden

I, Lukas Prader, agree that my bachelor's thesis ("Title"), supervised by Dr. Lauren Talluto, will be digitally archived in a repository of Leopold Franzens University Innsbruck and made available for further academic use.

Innsbruck, 22nd February 2024

Signature

University of Innsbruck

Faculty of Biology

Department of Ecology



Bachelor Thesis  
submitted for the degree of  
Bachelor of Science

**Studying SDM performance throughout a  
time series: A case study using the invasive  
species *Harmonia axyridis***

by  
Lukas Prader  
Matriculation Nr.: 12115058  
SE Biological Seminar: Ecology

Submission Date: 22nd February 2024  
Supervisors: Lauren Talluto, Gabriel Singer

## **Abstract**

  Lorem ipsum

# Contents

<b>1</b>	<b>Introduction</b>	<b>1</b>
<b>2</b>	<b>Materials and Methods</b>	<b>4</b>
2.1	Datasets . . . . .	4
2.2	Data preparation . . . . .	4
2.3	Model building . . . . .	6
2.4	Analysis . . . . .	6
<b>3</b>	<b>Results</b>	<b>7</b>
3.1	Temporal change of data availability . . . . .	7
3.2	Niche dynamic analysis . . . . .	7
3.3	SDMs, ensemble and time series . . . . .	9
<b>4</b>	<b>Discussion</b>	<b>12</b>
<b>5</b>	<b>Conclusion</b>	<b>12</b>
<b>6</b>	<b>Acknowledgements</b>	<b>12</b>
<b>A</b>	<b>Visualization of cleaned vs raw dataset</b>	<b>17</b>
<b>B</b>	<b>Niche analysis</b>	<b>17</b>
<b>C</b>	<b>Species distribution modelling</b>	<b>20</b>
<b>D</b>	<b>Model response curves</b>	<b>22</b>

# 1 Introduction

Invasive species are of special interest in ecological research due to their impact on native ecosystems. Main goals in this area are to find out which species have potential to become invasive, what habitat will be susceptible to invasion by those species, how fast the species will invade the new area and what impact its invasion will have on the native ecosystem<sup>1</sup>. To this end, many theories have been created to describe invasion processes. The invasion of a species can generally be described with four stages<sup>2</sup>:

1. Transport: Leaving the native range, arriving at a new location
2. Introduction: Existing in specific locations (captivity / cultivation)
3. Establishment: Existing outside of areas of introduction in the wild
4. Spread: Sustaining establishment and dispersing to new environments

Depending on the current stage there can be significant differences in behaviour and impact of a species. The impacts of invasive alien species can be numerous, ranging from food web changes to reductions in habitat and species richness, hydrology and nutrient cycle changes, enhanced invasion of other species and mass extinctions<sup>3</sup>. For example intraguild predation, the predation of species using similar resources, can create completely new stable states of an ecological system<sup>4</sup>. Fully understanding the dynamics at play during the invasion process would open more possibilities to actively influence the invasion of threatening species. For this, creating models which are able to predict the invasion is one current focus of research. Since invasion theory already uses niche theory, it is quite appropriate to think about applying niche models to the problem.

Species Distribution Models (SDMs), are being applied to predict the further development of species occurrences in many contexts, also for invasions. These types of models have been shown to generate substantial insight into the ecological requirements of species and, as niche models, can be used to predict the potential habitat of a species<sup>5</sup>. There has been considerable debate on the capabilities and limitations of SDMs, especially when used for prediction outside the data domain. In general, SDMs are made with the (ideal) assumption that the species is in environmental equilibrium<sup>6</sup>, implying that its ecological niche is not currently changing. If these models are now used to predict new, unsampled areas, there actually is no measure to assess their accuracy, since no data is presently available for that area<sup>5</sup>. This means that when trying to predict areas which are potentially outside the calibration range, sufficient validation data is lacking, implying strong uncertainty about the predictive performance of a given model<sup>5</sup>. This issue of model transferability is an

ongoing area of research in the SDM community. There is also no guarantee that the biotic interactions sampled in the study area will reflect the final interactions in the new area<sup>6</sup>. All of these issues apply especially to the prediction of invasive species, since there might be limited data in the invaded range, the species is often not currently at equilibrium and interactions with native species are completely new<sup>7</sup>. Despite all these challenges, SDMs have been used numerous times to provide insight into the invasive potential and the invasion dynamics of alien species<sup>8</sup>. One way of gaining more insight into the invasion process is to create models with data from different time periods during the invasion<sup>9</sup>. For example, data from a time period early in the invasion process can be used to build models which then are evaluated against data from a later time period<sup>10</sup>. With this, SDMs can be used to detect niche shifts, which in turn improves the understanding of the underlying niche dynamics and their impact, which helps to put model performance into perspective, for example when using its results for risk assessment of potential invasions<sup>11</sup>.

SDM performance is not only influenced by the underlying data, but also the type of model chosen for the analysis. Models range from regression methods to machine learning and each feature various strengths and weaknesses, possibly leading to vastly different results for the same dataset<sup>12</sup>. Due to those differences, a possible approach is to create an ensemble of multiple models<sup>13</sup>. The way of combining model predictions can vary, but the goal is to improve total performance by combining the results of all computed models.

In order to conduct an iterative modelling approach, a species with sufficient data over the time span of invasion is necessary. *Harmonia axyridis*, also known as the Harlequin ladybird or multicoloured Asian lady beetle, is of the family of the Coccinellidae and has its native origin in Asia<sup>14</sup>. At the time of download, the GBIF dataset for *H. axyridis* consisted of 468.462 data points globally, resulting in very sufficient amounts of data (see 3.1). At first widely introduced as a control species against pest aphids, *H. axyridis* has turned out to be a highly invasive species reaching an almost global distribution<sup>15</sup>. In America, the species was introduced as early as 1916 (California) and in 1988, first populations outside intended release were found<sup>16</sup>. Usage of *H. axyridis* for biological control in Europe dates back as far as 1990 (France)<sup>17</sup>. First invasive occurrences were confirmed in multiple countries during the early 2000s, including Germany (2000), Belgium (2001), the Netherlands (2002) and the United Kingdom (2003)<sup>14</sup>. The first confirmation in Austria, where it was never used for biological control, was in 2006<sup>18</sup>. It has been shown that all established invasive populations outside of North America have their origin in the first established population in eastern North America, with the European populations being significantly influenced by the used biocontrol strain<sup>19</sup>.

The impact of *H. axyridis* on invaded areas is diverse. In some contexts, the lady-

bird has been shown to have a negative impact on the diversity and abundance of native ladybird species<sup>14</sup>. Many studies show intra guild predation and direct inter-specific competition in favour of *H. axyridis*<sup>20</sup>. This results in a large potential for *H. axyridis* to be a significant threat for guild diversity and community structure in its introduced ranges. It has also been shown that the species feeds on a variety of damaged fruit crops, for example grapes, apples, stone fruit and berry crops, making it a pest in these scenarios<sup>21</sup>. The aggregating behaviour of *H. axyridis*, mostly as a strategy for overwintering, is also a cause of disturbance, since private homes and facilities are invaded by large amounts of beetles at a given time<sup>22</sup>. In general, *H. axyridis* can be concluded to be a species with high impact as an invader, and thus of interest for active research questions.

There have been several publications which modelled and predicted the distribution of *H. axyridis*, constrained to certain geographical ranges (i.e. Spain<sup>23</sup>, Chile<sup>24</sup>) or even on global scales<sup>25,26</sup>. There has not yet been any model iteration in form of a time series, which is what this thesis aims to add as new insight. Another goal of this thesis is to look into the limitations of models built early in the invasion process of a species. By iterating over the years of the invasion, model performance can be evaluated with consideration to the current state of invasion. In the end, a better understanding of the invasion process of *H. axyridis* in Europe and the performance of models trying to capture it should be the result.

## 2 Materials and Methods

This section elaborates on the Methods used to conduct this research.

### 2.1 Datasets

For occurrence data, all global occurrences of *H. axyridis* were downloaded from the GBIF database<sup>27</sup>. All traditional 19 bioclim variables were obtained from the CHELSA V2.1 climatologies dataset<sup>28,29</sup>, using the 1981-2010 time frame for all years from 2002 to 2010 as well as the MPI-ESM 1.2 ssp370 scenario 2011-2040 for all years from 2011 to 2022. As additional information, land cover data was used from the Copernicus Land cover Classification dataset<sup>30</sup> with yearly resolution for 2002 up to 2020.

### 2.2 Data preparation

All bioclim and land cover layers were resampled to a matching resolution of 30 arc seconds and cropped to two spatial extents, Europe and the presumed native range referencing (Orlova-Bienkowskaja, Ukrainsky & Brown, 2015)<sup>31</sup>.

The presence-only points from GBIF were checked for missing values for latitude, longitude, year or coordinate uncertainty and then subset to the afore mentioned spatial extents. No occurrences after 2022 were used, also no points with a coordinate uncertainty larger than 1 km. In Europe, the initial cut off year for presences was 1991, since this is the year of invasion according to the EASIN website. Afterwards, using the library CoordinateCleaner, all remaining data points were again checked for common errors or biases in the respective subset (tests used: "capitals", "centroids", "duplicates", "equal", "institutions", "outliers", "seas", "zeros"). In addition, all occurrences were checked for their land cover class values in their respective year, removing points in the water or with no data. In the end, remaining data points prior to 2002 were deemed insignificant and removed from the dataset. This resulted in a total of 124.746 presence points over all years and areas. To prepare the data for modelling, pseudoabsences were generated for each year, randomly sampling the area and resampling points in the water or with no data.

To correct for sampling bias in the data, the European and native extents were split into sub extents in order to add additional absences to denser sampled regions. For this, an algorithm was written which splits a given extent in half and continues to do so with the created sub-extents until the amount of points in the extents is at most some chosen number. For the first part of absence generation completely random absences are drawn from the original extent in order to ensure at least some coverage of the whole study area. In the second step, additional absences are gener-

ated for each subextent separately and in relation to the amount of presences inside the respective subextent. This results in more absences in regions with more presences as well (Fig. 1 A). The subdivision of the dataset was carried out using all presences in Europe over all years and setting the threshold to be  $\leq 30\%$ , leading to sub-extents converging around the United Kingdom and the Netherlands, which seem to have been sampled very intensely (Fig. 1 B). For the first and second step of absence generation, absences equal to and twice the amount of presences were generated respectively, resulting in three absences per presence in total.

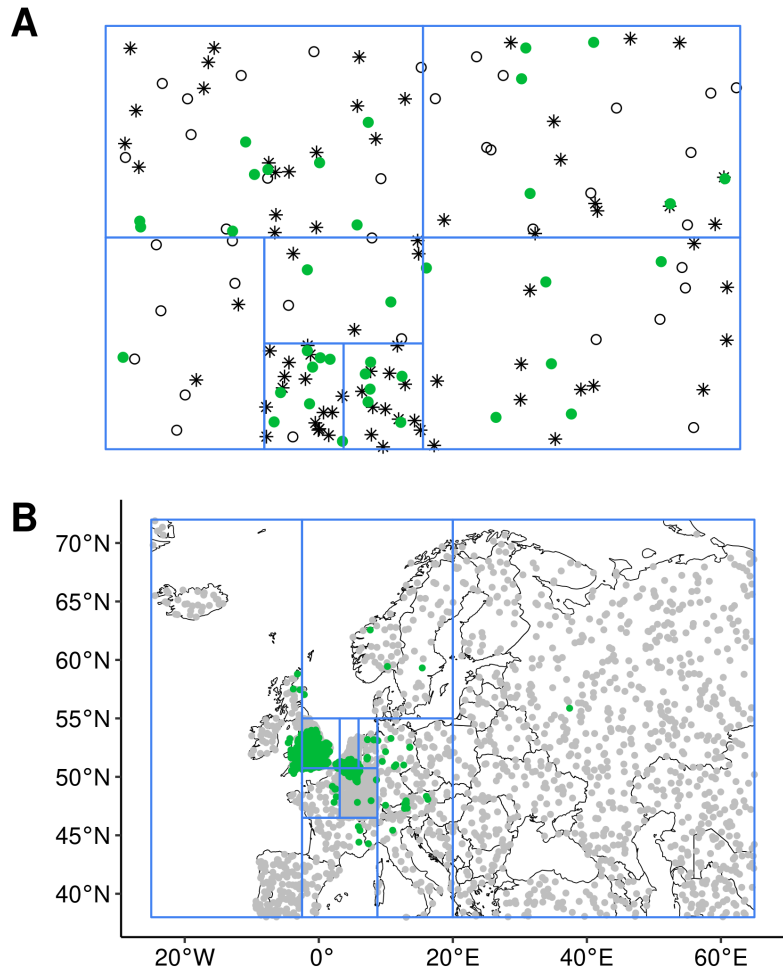


Figure 1: Visualization of the subdivision algorithm and absence generation. Sub-figure A shows an example of 30 generated presences (green), subdivided with a threshold of  $\leq 10$  points per subextent. The generated absences are shown in black, with circles indicating the first 30 completely random absences, and asterisks indicating absences generated relative to the amount of presences in a subextent. Sub-figure B shows the calculated subextents for the total presences of the dataset, with presences (green) and absences (grey) for 2008 plotted as an example.

## 2.3 Model building

For each year, the following Models were computed: General Linear (GLM)<sup>32</sup>, General Additive (GAM)<sup>32</sup>, Boosted Regression Trees (BRT)<sup>33</sup> and Maximum Entropy (MAXENT)<sup>34</sup>. A model for a specific year always included all points from past years as well. The iterative models that were built only use data points from Europe, though there was one model created only with native occurrences and predicted for each year in Europe. For all used occurrence points after 2020, the land cover data of 2020 was used as a substitute.

Variance inflation factors were used to select the variables used for model building. For this, a GAM was computed only using Europe data from 2002, using all bioclim and land cover variables. For land cover variables, a PCA was computed on the relative area of all land cover classes in an 18 km radius around 5000 random data points in Europe, subsequently projecting the occurrence data onto the resulting axes. The 18 km radius was chosen, since it is the average flight distance determined for *H. axyridis*<sup>35</sup>. PCA axes were included in the model until a cut-off of 80% of explained variance was reached. Variance inflation factors were computed for this GAM and the variable with the highest VIF was dropped until none of the remaining variables had a VIF greater than 10.

## 2.4 Analysis

All SDM models of each year were evaluated for their accuracy on predicting the occurrences of the following year using the Sensitivity or True Positive Rate (TPR). The TPR values were used to create a TPR-weighted ensemble of all model predictions, which was again evaluated for its accuracy. The thresholds used to compute TPR were computed using the library `PresenceAbsence` while maximizing  $(\text{sens} + \text{spec}) / 2$ . This thresholding was chosen since just maximizing TPR can be achieved trivially by setting the threshold as low as possible, creating a model which predicts everything as suitable (used thresholds in Supplementary Tab. 6). For each year, the occupied niche was computed by running a PCA analysis on the bioclim variables. The niche was then visualized by plotting a dynamic occurrence density grid for the first two PCA axes<sup>36</sup>. The overlap between each year for Europe and the respective following year was computed, as well as the niche dynamic indices "stability", "expansion" and "unfilling"<sup>37</sup>. Niche overlap for the total EU data was also visualized in comparison to the total native niche. All mentioned niche analyses were conducted using the library `ecospat`<sup>38</sup>. The development of TPR over time was tested for correlation with the amount of training data and the niche stability for a given year, using the Pearson correlation test.

### 3 Results

The analyses mentioned above resulted in findings which shed light on the niche dynamics and predictability of *H. axyridis*.

#### 3.1 Temporal change of data availability

Taking the amount of presence points in Europe and the native range, one can plot the amount of presences available for each year respectively (Fig. 2).

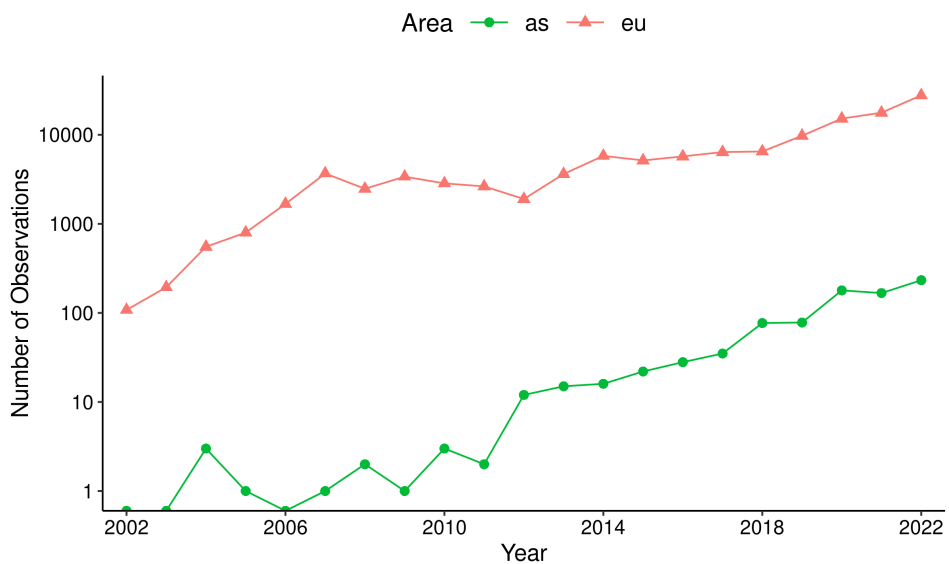


Figure 2: Amount of presence points for *H. axyridis* by year and area, using the cleaned dataset (Supplementary Fig. 8).

The resulting figure shows that the amount of data available in the invaded range greatly surpasses the amount in the native range. With at least 100 presences for any year, the European dataset is definitely sufficient to create SDMs for each year separately, more so if data from previous years is also used. The exponential increase in observations over time also suggests rapid population growth. The lack of presence points in early years in the native range was the reason why it was decided to only create one SDM with the native data of all years combined, since it is more likely to provide a complete evaluation of the native niche.

#### 3.2 Niche dynamic analysis

When comparing the total native and invaded niches (so all years included), the niches are clearly different (Fig. 3). A niche similarity test produced a p value of  $p = 0.32$ , leading to an accepted null hypothesis meaning the two niches are not more similar than random (Supplementary Fig. 9). Conducting a niche equivalency

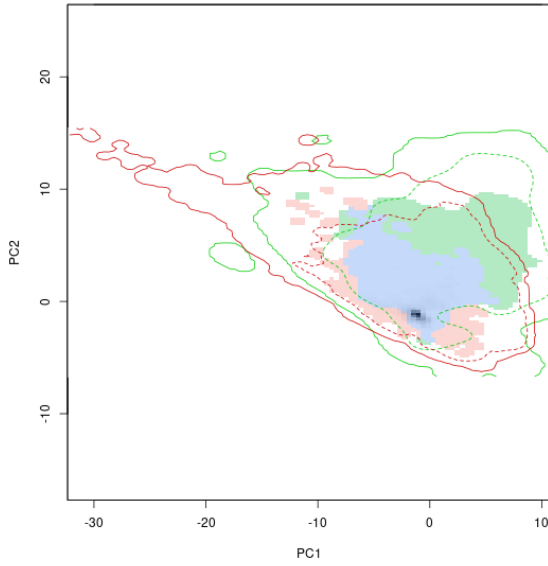


Figure 3: Native (green) and invaded (red) niche of *H. axyridis*, shown along the first two axes of a PCA using all bioclim variables (Supplementary Fig. 10). The blue area indicates overlap between the occupied niches. Dashed and solid lines indicate 50% and 100% of the potentially available environment in each area (from background). Grey shading shows the density distribution of the invaded niche.

test, the result was  $p = 0.01$  implying highly significant differences between the two niches (Supplementary Fig. 9).

Looking at the niche only in the invaded range, one can visualize the shift and expansion throughout the years (Fig. 4).

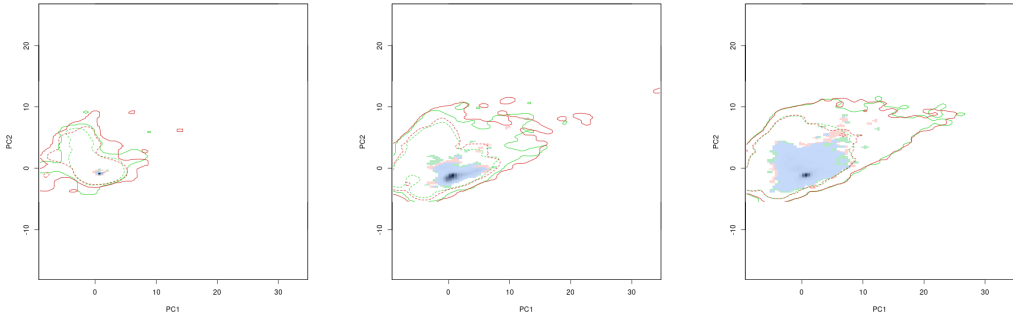


Figure 4: The progression of the invaded niche of *H. axyridis*, shown along the first two axes of a PCA using all bioclim variables (Supplementary Fig. 11). Niches of the years (from left to right) 2002, 2012 and 2021 compared to the niche of their following years respectively. Green shows the first year, red shows the year after and blue indicates overlap. Dashed and solid lines indicate 50% and 100% of the potentially available environment (from background). Grey shading shows the density distribution of the second year.

In addition to a visualization, it makes sense to compute the niche dynamic in-

dices<sup>37</sup>, as well as the niche overlap (Schoener's D) for each year in order to characterize the niche shift further (Fig. 5).

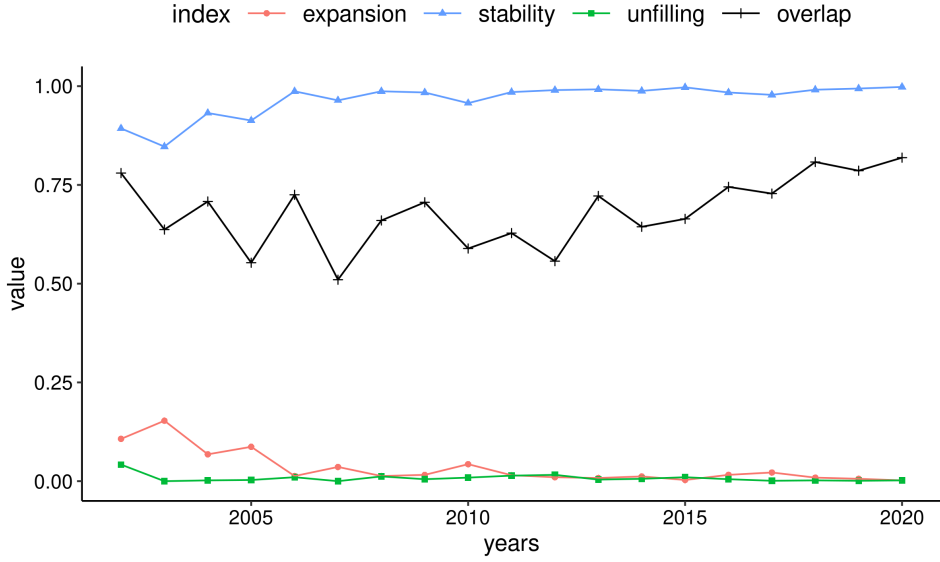


Figure 5: Niche dynamic indices and overlap (Schoener's D) computed from comparing each year of the invaded niche of *H. axyridis* to the following year.

The results show that in the first five years of the time series, the invaded niche is still expanding, while afterwards it becomes almost completely stable. Once stability is reached, *H. axyridis* seems to just fill out the rest of the acquired niche, as shown by an increase in niche overlap.

### 3.3 SDMs, ensemble and time series

Variable selection using VIFs resulted in 13 variables, which were used for modelling (Tab. 1).

Table 1: Final 13 variables resulting from variable selection with VIFs, PCA contribution table for all land cover variables in (Supplementary Tab. 4).

Name	lc1	lc2	lc4	lc6	bio10	bio13	bio14	bio15	bio18	bio3	bio6	bio8	bio9
VIF	8.18	5.2	4.93	4.56	4.81	7.96	6.3	7.58	3.34	4.64	5.94	2.63	1.92

After computing all of the mentioned models (response curves in appendix D) and creating a TPR weighted ensemble, one can examine the development over time in more detail (Fig. 6).

The difference in performance between the invaded and native range models is apparent, with the invaded range models achieving a higher TPR on average. Surprisingly, the invasive data models already perform very well in the first years and continue to do so for all further years. It is notable, that the GLM almost always performs the best out of all native models.

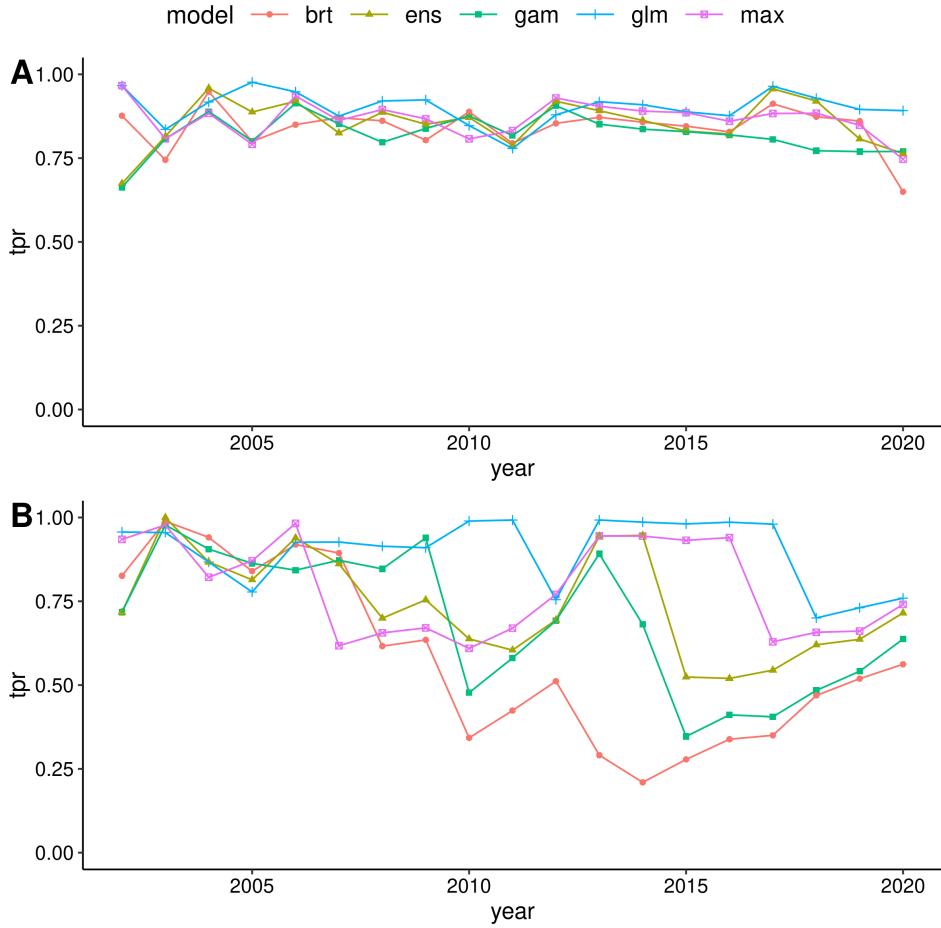


Figure 6: SDM predictive performance over time. Subfigure A shows the performance of models created with invasive data up to the year in question in predicting the following year. Subfigure B shows the performance of models created with all the native data in predicting the year in question.

Trying to correlate the performance of each model individually to the trend in data amount or the niche stability value lead to statistically insignificant results for all models (Tab. 2).

Table 2: Results when correlating model TPR to either niche stability or amount of data.

Model	glm	gam	brt	max	ens
<b>Corr. niche stability</b>	-0.036	0.278	0.072	0.122	0.253
<b>p-value</b>	0.885	0.249	0.771	0.619	0.296
<b>Corr. data count</b>	-0.044	-0.27	-0.296	-0.32	-0.083
<b>p-value</b>	0.858	0.263	0.219	0.181	0.735

In the end, one can look at the model predictions for the year 2022 and compare them to the observed presences of that year (Fig. 7).

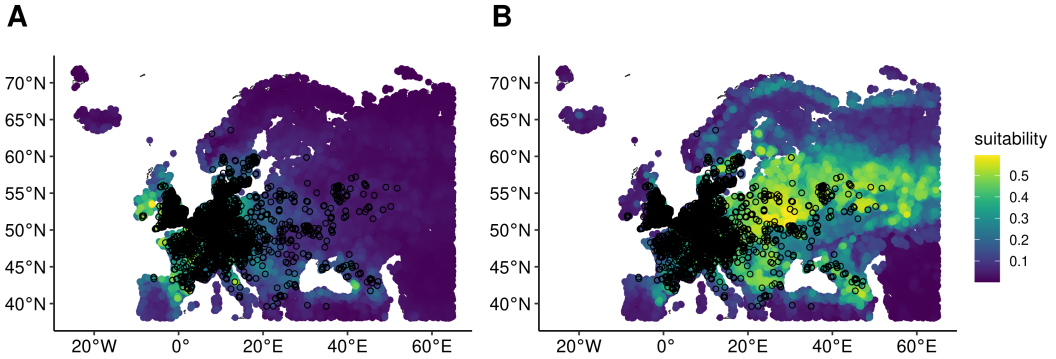


Figure 7: Predictions of the invaded (A) and native data (B) ensemble models for the suitability of *H. axyridis* in 2022. Suitability shown as colour, black circles indicating presences observed in 2022.

The ensemble from the invaded range proves to be more accurate in predicting the presences of 2022, although being rather conservative in its predictions. The native ensemble predicts a much wider range in comparison, reaching much further to the east.

## **4 Discussion**

## **5 Conclusion**

## **6 Acknowledgements**

## References

1. Shigesada, N. & Kawasaki, K. *Biological invasions: theory and practice* [https://books.google.at/books/about/Biological\\_Invasions\\_Theory\\_and\\_Practice.html?id=Ri-hle\\_zdpsc&redir\\_esc=y](https://books.google.at/books/about/Biological_Invasions_Theory_and_Practice.html?id=Ri-hle_zdpsc&redir_esc=y) (Oxford University Press, UK, 1997).
2. Blackburn, T. M. *et al.* A proposed unified framework for biological invasions. *Trends in ecology & evolution* **26**, 333–339. doi:10.1016/j.tree.2011.03.023 (2011).
3. Simberloff, D. *et al.* Impacts of biological invasions: what's what and the way forward. *Trends in ecology & evolution* **28**, 58–66. doi:10.1016/j.tree.2012.07.013 (2013).
4. Polis, G. A., Myers, C. A. & Holt, R. D. The ecology and evolution of intraguild predation: potential competitors that eat each other. *Annual review of ecology and systematics* **20**, 297–330. doi:10.1146/annurev.es.20.110189.001501 (1989).
5. Araújo, M. B. & Guisan, A. Five (or so) challenges for species distribution modelling. *Journal of biogeography* **33**, 1677–1688. doi:10.1111/j.1365-2699.2006.01584.x (2006).
6. Elith, J. & Leathwick, J. R. Species distribution models: ecological explanation and prediction across space and time. *Annual review of ecology, evolution, and systematics* **40**, 677–697. doi:10.1146/annurev.ecolsys.110308.120159 (2009).
7. Mainali, K. P. *et al.* Projecting future expansion of invasive species: comparing and improving methodologies for species distribution modeling. *Global change biology* **21**, 4464–4480. doi:10.1111/gcb.13038 (2015).
8. Zimmermann, N. E., Edwards Jr, T. C., Graham, C. H., Pearman, P. B. & Svenning, J.-C. New trends in species distribution modelling. *Ecography* **33**, 985–989. doi:10.1111/j.1600-0587.2010.06953.x (2010).
9. Briscoe Runquist, R. D., Lake, T., Tiffin, P. & Moeller, D. A. Species distribution models throughout the invasion history of Palmer amaranth predict regions at risk of future invasion and reveal challenges with modeling rapidly shifting geographic ranges. *Scientific Reports* **9**, 2426. doi:10.1038/s41598-018-38054-9 (2019).
10. Barbet-Massin, M., Rome, Q., Villemant, C. & Courchamp, F. Can species distribution models really predict the expansion of invasive species? *PloS one* **13**, e0193085. doi:10.1371/journal.pone.0193085 (2018).
11. Pearman, P. B., Guisan, A., Broennimann, O. & Randin, C. F. Niche dynamics in space and time. *Trends in ecology & evolution* **23**, 149–158. doi:10.1016/j.tree.2007.11.005 (2008).

12. Valavi, R., Guillera-Arroita, G., Lahoz-Monfort, J. J. & Elith, J. Predictive performance of presence-only species distribution models: a benchmark study with reproducible code. *Ecological Monographs* **92**, e01486. doi:10.1002/ecm.1486 (2022).
13. Araújo, M. B. & New, M. Ensemble forecasting of species distributions. *Trends in ecology & evolution* **22**, 42–47. doi:10.1016/j.tree.2006.09.010 (2007).
14. Roy, H. E. *et al.* The harlequin ladybird, *Harmonia axyridis*: global perspectives on invasion history and ecology. *Biological invasions* **18**, 997–1044. doi:10.1007/s10530-016-1077-6 (2016).
15. Brown, P. *et al.* *Harmonia axyridis* in Europe: spread and distribution of a non-native coccinellid. *BioControl* **53**, 5–21. doi:10.1007/s10526-007-9132-y (2008).
16. Chapin, J. B., Brou, V. *et al.* *Harmonia axyridis* (Pallas), the third species of the genus to be found in the United States (Coleoptera: Coccinellidae). *Proc. Entomol. Soc. Wash* **93**, 630–635. <https://www.biodiversitylibrary.org/partpdf/55539> (1991).
17. Coutanceau, J. *Harmonia axyridis* (Pallas, 1773): Une coccinelle asiatique introduite, acclimatée et en extension en France. *Bulletin de la Société Entomologique de France* **111**, 395–401. doi:10.3406/bsef.2006.16343 (Jan. 2006).
18. Rabitsch, W. & Schuh, R. First record of the multicoloured Asian ladybird *Harmonia axyridis* (Pallas, 1773) in Austria. *Beiträge zur Entomofaunistik* **7**, 161–164. [https://www.zobodat.at/pdf/BEF\\_7\\_0161-0164.pdf](https://www.zobodat.at/pdf/BEF_7_0161-0164.pdf) (2006).
19. Lombaert, E. *et al.* Bridgehead effect in the worldwide invasion of the biocontrol harlequin ladybird. *PloS one* **5**, e9743. doi:10.1371/journal.pone.0009743 (2010).
20. Pell, J. K., Baverstock, J., Roy, H. E., Ware, R. L. & Majerus, M. E. Intraguild predation involving *Harmonia axyridis*: a review of current knowledge and future perspectives. *BioControl* **53**, 147–168. doi:10.1007/978-1-4020-6939-0\_10 (2008).
21. Koch, R., Burkness, E., Burkness, S. W. & Hutchison, W. Phytophagous preferences of the multicolored Asian lady beetle (Coleoptera: Coccinellidae) for autumn-ripening fruit. *Journal of Economic Entomology* **97**, 539–544. doi:10.1093/jee/97.2.539 (2004).
22. Nalepa, C., Kennedy, G. & Brownie, C. Role of visual contrast in the alighting behavior of *Harmonia axyridis* (Coleoptera: Coccinellidae) at overwintering sites. *Environmental Entomology* **34**, 425–431. doi:10.1603/0046-225X-34.2.425 (2005).
23. Ameixa, O. M., Šipoš, J., Burda, M., Soares, A. M. & Soares, A. O. Factors influencing the introduction and spread of *Harmonia axyridis* in the Iberian Peninsula. *Biological Invasions* **21**, 323–331. doi:10.1007/s10530-018-1841-x (2019).

24. Alaniz, A., Grez, A. & Zaviezo, T. Potential spatial interaction of the invasive species *Harmonia axyridis* (Pallas) with native and endemic coccinellids. *Journal of Applied Entomology* **142**, 513–524. doi:10.1111/jen.12498 (2018).
25. Bidinger, K., Lötters, S., Rödder, D. & Veith, M. Species distribution models for the alien invasive Asian Harlequin ladybird (*Harmonia axyridis*). *Journal of Applied Entomology* **136**, 109–123. doi:10.1111/j.1439-0418.2010.01598.x (2012).
26. Poutsma, J., Loomans, A., Aukema, B. & Heijerman, T. Predicting the potential geographical distribution of the harlequin ladybird, *Harmonia axyridis*, using the CLIMEX model. *From Biological Control to Invasion: the ladybird Harmonia axyridis as a model species*, 103–125. doi:10.1007/s10526-007-9140-y (2008).
27. Gbif.org. GBIF Occurrence Download 15th July 2023. doi:10.15468/dl.y4y3s9.
28. Karger, D. N. *et al.* Climatologies at high resolution for the earth's land surface areas. *Scientific data* **4**, 1–20. doi:10.1038/sdata.2017.122 (2017).
29. Karger, D. N. *et al.* *Climatologies at high resolution for the earth's land surface areas* (Last accessed 3 August 2023). 2021. doi:10.16904/envidat.228.
30. Copernicus Climate Change Service. *Land cover classification gridded maps from 1992 to present derived from satellite observation* (Last accessed 3 August 2023). 2019. doi:10.24381/cds.006f2c9a.
31. Orlova-Bienkowskaja, M. J., Ukrainsky, A. S. & Brown, P. M. *Harmonia axyridis* (Coleoptera: Coccinellidae) in Asia: a re-examination of the native range and invasion to southeastern Kazakhstan and Kyrgyzstan. *Biological Invasions* **17**, 1941–1948. doi:10.1007/s10530-015-0848-9 (2015).
32. Guisan, A., Edwards Jr, T. C. & Hastie, T. Generalized linear and generalized additive models in studies of species distributions: setting the scene. *Ecological modelling* **157**, 89–100. doi:10.1016/S0304-3800(02)00204-1 (2002).
33. Elith, J., Leathwick, J. R. & Hastie, T. A working guide to boosted regression trees. *Journal of animal ecology* **77**, 802–813. doi:10.1111/j.1365-2656.2008.01390.x (2008).
34. Phillips, S. J., Anderson, R. P., Dudík, M., Schapire, R. E. & Blair, M. E. Opening the black box: An open-source release of Maxent. *Ecography* **40**, 887–893. doi:10.1111/ecog.03049 (2017).
35. Jeffries, D. L. *et al.* Characteristics and drivers of high-altitude ladybird flight: insights from vertical-looking entomological radar. *PloS one* **8**, e82278. doi:10.1371/journal.pone.0082278 (2013).
36. Broennimann, O. *et al.* Measuring ecological niche overlap from occurrence and spatial environmental data. *Global ecology and biogeography* **21**, 481–497. doi:10.1111/j.1466-8238.2011.00698.x (2012).

37. Guisan, A., Petitpierre, B., Broennimann, O., Daehler, C. & Kueffer, C. Unifying niche shift studies: insights from biological invasions. *Trends in ecology & evolution* **29**, 260–269. doi:10.1016/j.tree.2014.02.009 (2014).
38. Di Cola, V. *et al.* ecospat: an R package to support spatial analyses and modeling of species niches and distributions. *Ecography* **40**, 774–787. doi:10.1111/ecog.02671 (2017).

## A Visualization of cleaned vs raw dataset

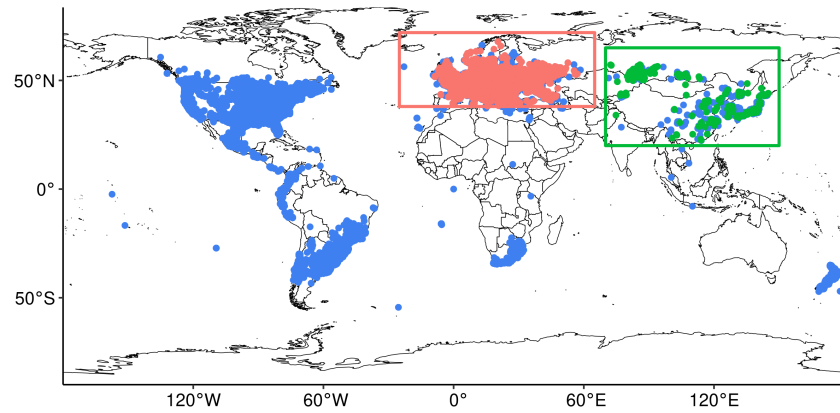


Figure 8: Visualization of the cleaned dataset for *H. axyridis* in comparison to the total raw dataset. The red and green boxes show the used extents for Europe and the native range respectively, red and green points show the cleaned presence points in their respective extents, while blue points show all points of the raw dataset.

## B Niche analysis

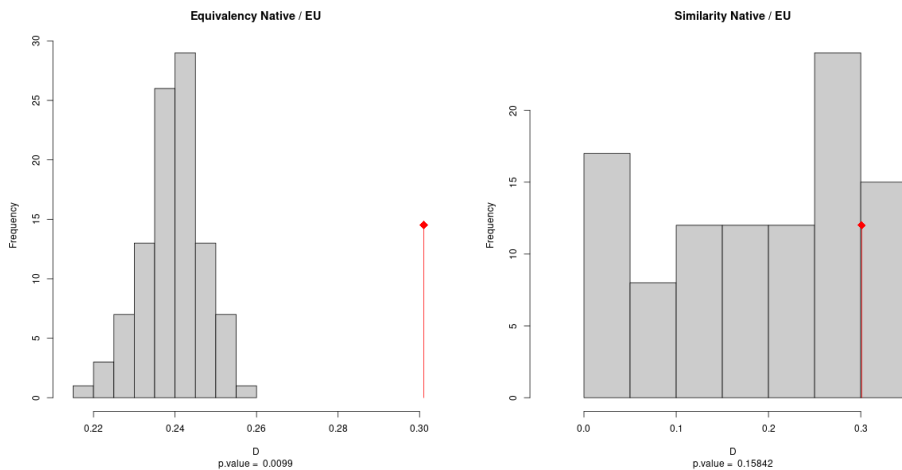


Figure 9: Results of the niche equivalency (left) and niche similarity (right) test comparing the native and invaded niche of *H. axyridis*. Histograms of the simulated niche overlaps, the observed overlap shown as a red bar with a diamond.

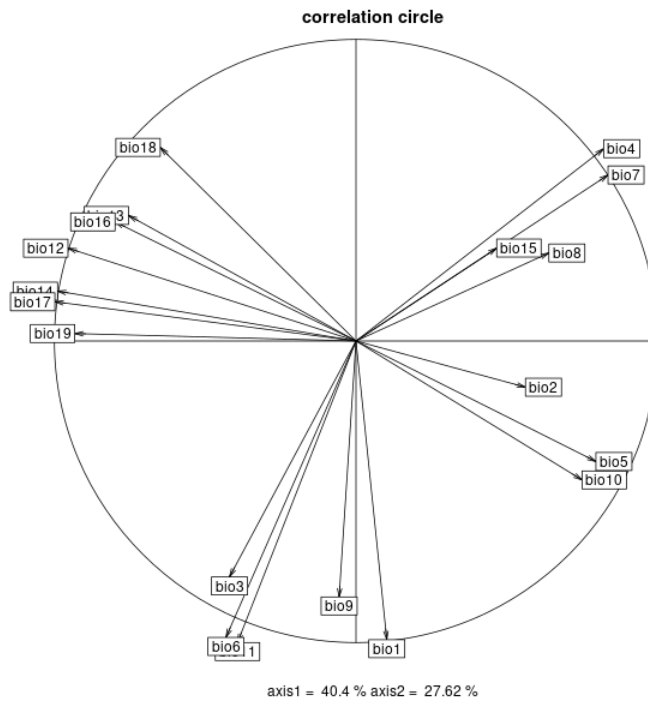


Figure 10: Component contributions for the PCA used to conduct the niche analyses comparing the total native and invaded niches. For detail on the bioclim variables, see (Supplementary Tab. 3).

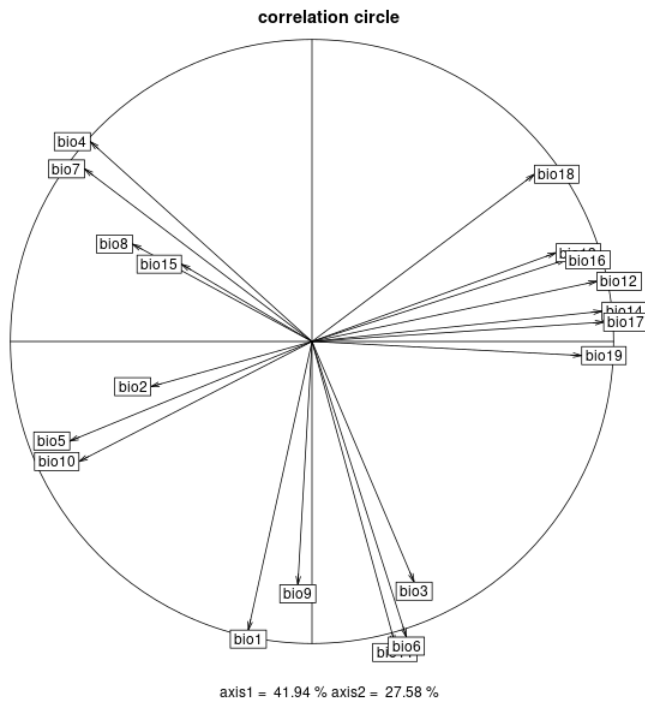


Figure 11: Component contributions for the PCA used to conduct the niche analyses comparing each year of the invaded niche to its following year. For detail on the bioclim variables, see (Supplementary Tab. 3).

Table 3: Explanation of the bioclim variables (from CHELSA 2.x technical specifications).

<b>Variable</b>	<b>Explanation</b>
bio1	mean annual air temperature
bio2	mean diurnal air temperature range
bio3	isothermality
bio4	temperature seasonality
bio5	mean daily maximum air temperature of the warmest month
bio6	mean daily minimum air temperature of the coldest month
bio7	annual range of air temperature
bio8	mean daily mean air temperatures of the wettest quarter
bio9	mean daily mean air temperatures of the driest quarter
bio10	mean daily mean air temperatures of the warmest quarter
bio11	mean daily mean air temperatures of the coldest quarter
bio12	annual precipitation amount
bio13	precipitation amount of the wettest month
bio14	precipitation amount of the driest month
bio15	precipitation seasonality
bio16	mean monthly precipitation amount of the wettest quarter
bio17	mean monthly precipitation amount of the driest quarter
bio18	mean monthly precipitation amount of the warmest quarter
bio19	mean monthly precipitation amount of the coldest quarter

## C Species distribution modelling

Table 4: Table showing PCA contributions for each Copernicus land cover class, Copernicus land cover class explanation in (Supplementary Tab. 5).

Class	lc1	lc2	lc3	lc4	lc5	lc6
0	$7.67 \times 10^{-34}$	$2.90 \times 10^{-34}$	$9.09 \times 10^{-34}$	$6.84 \times 10^{-35}$	$3.13 \times 10^{-34}$	$1.35 \times 10^{-36}$
10	$4.34 \times 10^1$	$1.71 \times 10^1$	$2.27 \times 10^1$	$5.36 \times 10^{-1}$	7.00	$4.36 \times 10^{-1}$
11	6.41	$7.20 \times 10^{-1}$	5.86	8.10	$6.54 \times 10^1$	$4.62 \times 10^{-1}$
12	$1.67 \times 10^{-3}$	$6.40 \times 10^{-6}$	$1.53 \times 10^{-2}$	$6.85 \times 10^{-5}$	$6.96 \times 10^{-2}$	$2.52 \times 10^{-2}$
20	$2.95 \times 10^{-3}$	$1.32 \times 10^{-1}$	$2.58 \times 10^{-4}$	$2.28 \times 10^{-2}$	$6.36 \times 10^{-2}$	$2.97 \times 10^{-3}$
30	$3.54 \times 10^{-1}$	$4.06 \times 10^{-2}$	$4.35 \times 10^{-1}$	$5.83 \times 10^{-1}$	$3.13 \times 10^{-2}$	$3.80 \times 10^{-1}$
40	$8.36 \times 10^{-2}$	$5.08 \times 10^{-3}$	$3.07 \times 10^{-1}$	$9.58 \times 10^{-5}$	$2.46 \times 10^{-1}$	$1.05 \times 10^{-1}$
50	0.00	$3.01 \times 10^{-34}$	$4.81 \times 10^{-33}$	$2.77 \times 10^{-30}$	$7.70 \times 10^{-32}$	$1.23 \times 10^{-30}$
60	$1.84 \times 10^{-1}$	$4.91 \times 10^{-1}$	6.49	$6.12 \times 10^1$	$3.45 \times 10^{-3}$	1.31
61	$1.21 \times 10^{-4}$	$6.93 \times 10^{-5}$	$4.19 \times 10^{-6}$	$1.43 \times 10^{-3}$	$9.89 \times 10^{-5}$	$5.24 \times 10^{-5}$
62	$4.04 \times 10^{-41}$	$1.84 \times 10^{-38}$	$4.23 \times 10^{-35}$	0.00	0.00	$1.23 \times 10^{-30}$
70	$4.59 \times 10^1$	$2.44 \times 10^1$	6.62	3.54	$5.85 \times 10^{-3}$	2.85
71	$5.64 \times 10^{-11}$	$9.17 \times 10^{-11}$	$1.12 \times 10^{-11}$	$1.25 \times 10^{-11}$	$4.80 \times 10^{-11}$	$4.79 \times 10^{-10}$
72	0.00	$2.74 \times 10^{-46}$	0.00	$1.84 \times 10^{-38}$	$4.59 \times 10^{-39}$	$3.01 \times 10^{-34}$
80	$1.41 \times 10^{-5}$	$6.90 \times 10^{-7}$	$9.66 \times 10^{-10}$	$1.76 \times 10^{-6}$	$2.09 \times 10^{-7}$	$7.78 \times 10^{-6}$
81	$3.98 \times 10^{-57}$	$2.61 \times 10^{-52}$	$4.28 \times 10^{-48}$	0.00	0.00	$7.35 \times 10^{-38}$
82	0.00	0.00	$4.18 \times 10^{-51}$	$6.84 \times 10^{-47}$	$6.84 \times 10^{-47}$	$7.17 \times 10^{-41}$
90	1.05	$6.90 \times 10^{-1}$	$3.31 \times 10^{-1}$	8.27	$2.01 \times 10^{-2}$	$7.52 \times 10^{-1}$
100	$8.89 \times 10^{-2}$	$2.08 \times 10^{-2}$	$9.54 \times 10^{-2}$	$3.51 \times 10^{-2}$	$2.48 \times 10^{-2}$	$4.78 \times 10^{-2}$
110	$1.82 \times 10^{-2}$	$4.76 \times 10^{-3}$	$1.07 \times 10^{-2}$	$4.45 \times 10^{-3}$	$1.82 \times 10^{-2}$	$2.46 \times 10^{-1}$
120	$1.10 \times 10^{-2}$	$3.53 \times 10^{-1}$	$6.47 \times 10^{-2}$	$2.27 \times 10^{-4}$	$7.52 \times 10^{-3}$	$1.53 \times 10^{-1}$
121	$1.32 \times 10^{-80}$	$3.45 \times 10^{-75}$	0.00	$2.37 \times 10^{-64}$	$9.50 \times 10^{-64}$	$1.02 \times 10^{-54}$
122	$1.56 \times 10^{-2}$	$1.31 \times 10^{-2}$	$3.05 \times 10^{-3}$	$3.08 \times 10^{-3}$	$4.34 \times 10^{-3}$	$6.71 \times 10^{-1}$
130	$2.88 \times 10^{-1}$	3.07	$2.67 \times 10^1$	$1.60 \times 10^1$	$2.21 \times 10^1$	$1.94 \times 10^1$
140	$1.12 \times 10^{-4}$	$5.70 \times 10^{-3}$	$6.71 \times 10^{-4}$	$1.30 \times 10^{-3}$	$3.27 \times 10^{-3}$	$4.87 \times 10^{-2}$
150	$1.31 \times 10^{-1}$	4.39	$2.93 \times 10^{-1}$	1.30	3.45	$5.20 \times 10^1$
151	$3.00 \times 10^{-93}$	$1.23 \times 10^{-89}$	$1.81 \times 10^{-84}$	$6.81 \times 10^{-81}$	$1.08 \times 10^{-80}$	$5.53 \times 10^{-74}$
152	$2.53 \times 10^{-4}$	$3.69 \times 10^{-5}$	$1.65 \times 10^{-5}$	$2.25 \times 10^{-5}$	$5.64 \times 10^{-6}$	$2.87 \times 10^{-4}$
153	$2.57 \times 10^{-5}$	$1.70 \times 10^{-5}$	$1.49 \times 10^{-5}$	$8.04 \times 10^{-5}$	$2.01 \times 10^{-5}$	$1.54 \times 10^{-4}$
160	$5.97 \times 10^{-5}$	$1.07 \times 10^{-4}$	$1.04 \times 10^{-4}$	$2.47 \times 10^{-5}$	$4.30 \times 10^{-5}$	$4.22 \times 10^{-4}$
170	0.00	0.00	0.00	0.00	0.00	0.00
180	1.28	$2.45 \times 10^{-1}$	$3.66 \times 10^{-2}$	$1.77 \times 10^{-2}$	$3.78 \times 10^{-2}$	$2.67 \times 10^{-1}$
190	$3.76 \times 10^{-2}$	$7.01 \times 10^{-3}$	$2.54 \times 10^{-2}$	$2.14 \times 10^{-2}$	$1.18 \times 10^{-1}$	$7.56 \times 10^{-3}$
200	$5.52 \times 10^{-1}$	$4.83 \times 10^1$	$3.00 \times 10^1$	$1.53 \times 10^{-1}$	1.39	9.21
201	$4.02 \times 10^{-5}$	$9.95 \times 10^{-6}$	$1.26 \times 10^{-4}$	$6.16 \times 10^{-8}$	$1.47 \times 10^{-4}$	$6.12 \times 10^{-5}$
202	$1.90 \times 10^{-4}$	$1.61 \times 10^{-2}$	$8.83 \times 10^{-3}$	$8.67 \times 10^{-5}$	$5.88 \times 10^{-4}$	$1.87 \times 10^{-3}$
210	$2.50 \times 10^{-1}$	$1.19 \times 10^{-2}$	$1.47 \times 10^{-2}$	$2.43 \times 10^{-1}$	$8.46 \times 10^{-6}$	$1.16 \times 10^1$
220	$1.87 \times 10^{-4}$	$4.15 \times 10^{-3}$	$2.22 \times 10^{-7}$	$1.12 \times 10^{-5}$	$5.05 \times 10^{-4}$	$1.48 \times 10^{-2}$

Table 5: Explanation of the Copernicus land cover classes (from dataset legend).

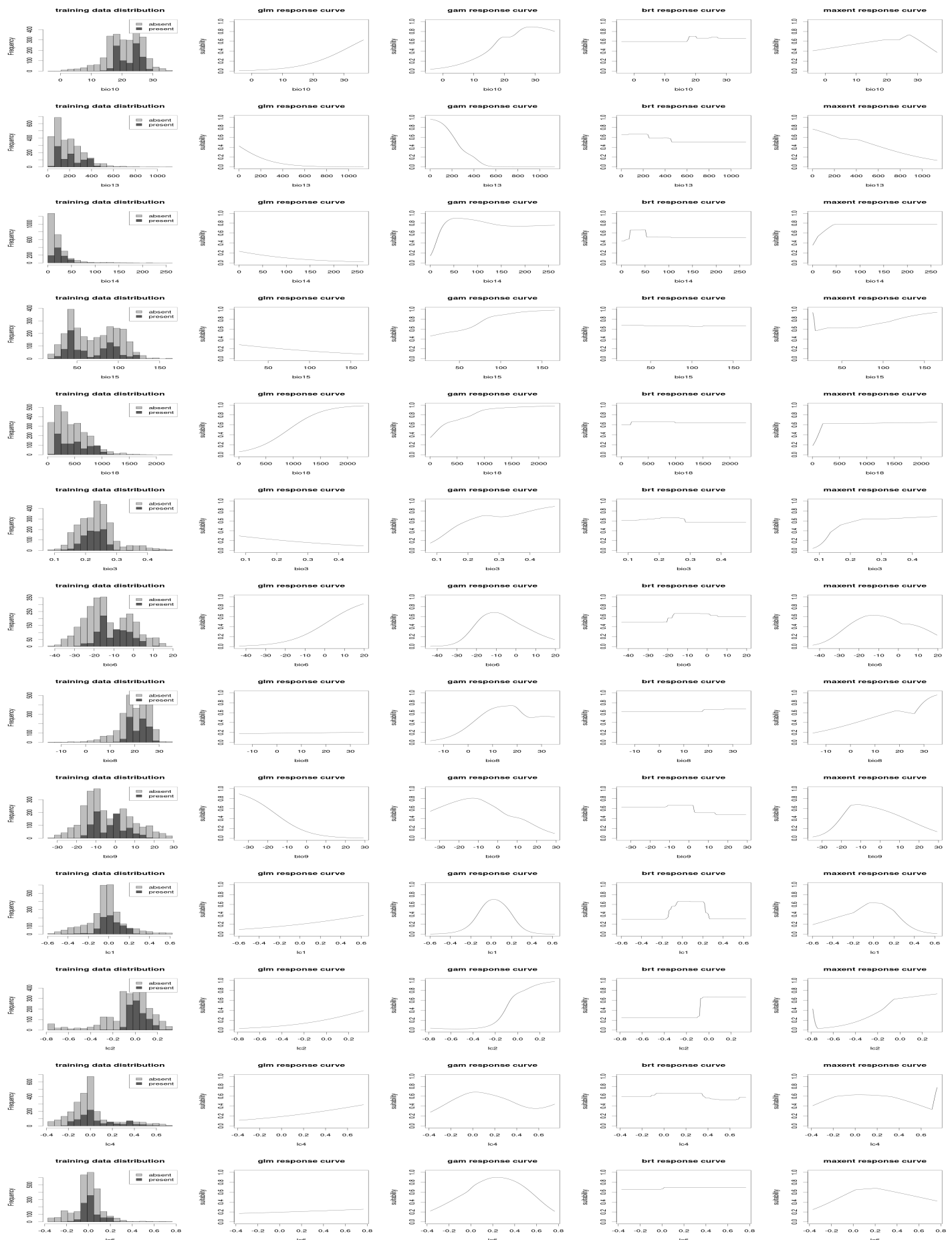
<b>Class</b>	<b>Explanation</b>
0	no data
10	cropland rainfed
11	cropland rainfed herbaceous cover
12	cropland rainfed tree or shrub cover
20	cropland irrigated
30	mosaic cropland
40	mosaic natural vegetation
50	tree broadleaved evergreen closed to open
60	tree broadleaved deciduous closed to open
61	tree broadleaved deciduous closed
62	tree broadleaved deciduous open
70	tree needleleaved evergreen closed to open
71	tree needleleaved evergreen closed
72	tree needleleaved evergreen open
80	tree needleleaved deciduous closed to open
81	tree needleleaved deciduous closed
82	tree needleleaved deciduous open
90	tree mixed
100	mosaic tree and shrub
110	mosaic herbaceous
120	shrubland
121	shrubland evergreen
122	shrubland deciduous
130	grassland
140	lichens and mosses
150	sparse vegetation
151	sparse tree
152	sparse shrub
153	sparse herbaceous
160	tree cover flooded fresh or brakish water
170	tree cover flooded saline water
180	shrub or herbaceous cover flooded
190	urban
200	bare areas
201	bare areas consolidated
202	bare areas unconsolidated
210	water
220	snow and ice

Table 6: Thresholds used to predict the models for the given years (inv = invaded range model (of the previous year), nat = native range model).

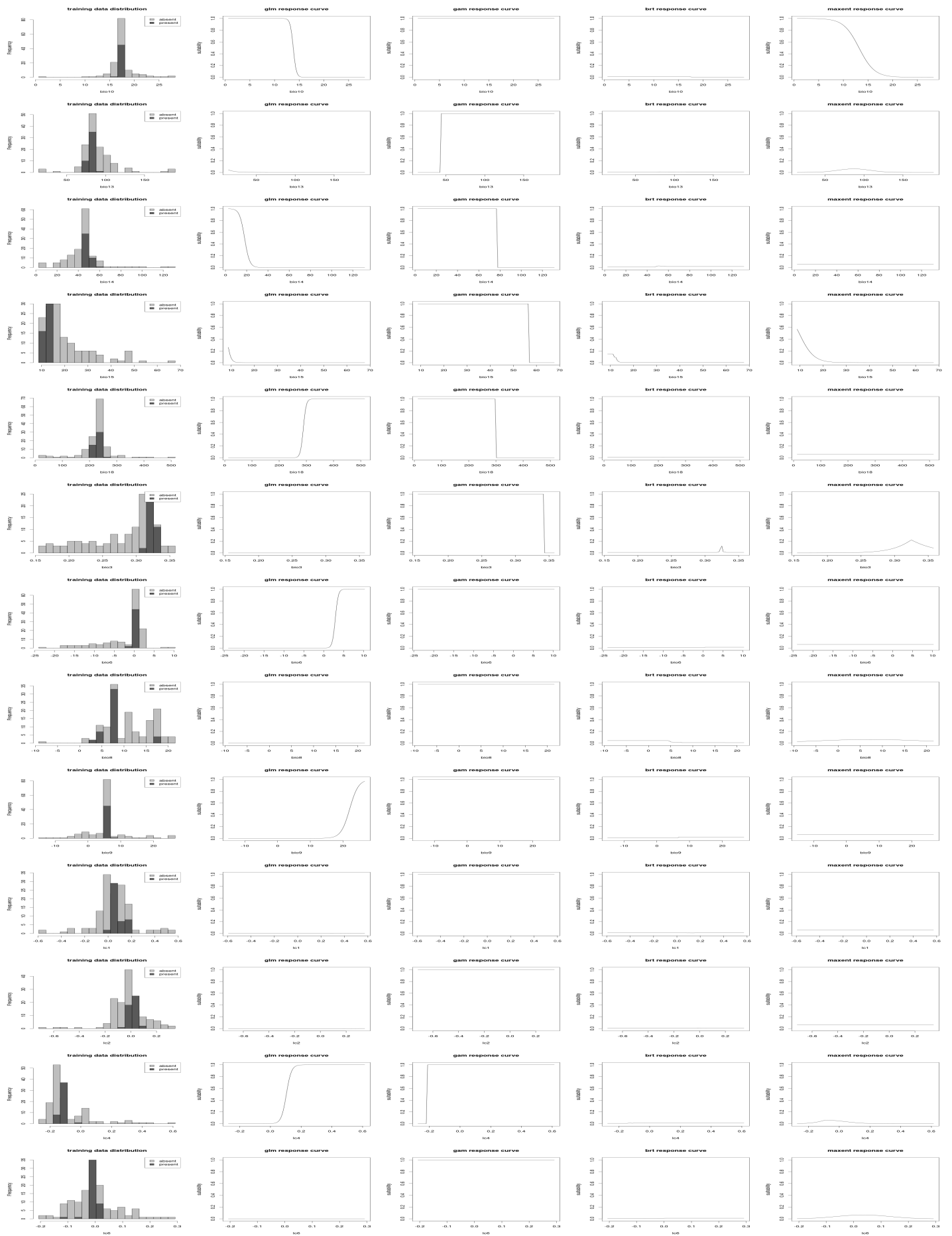
<b>Year</b>	<b>glm inv</b>	<b>gam inv</b>	<b>brt inv</b>	<b>max inv</b>	<b>ens inv</b>	<b>glm nat</b>	<b>gam nat</b>	<b>brt nat</b>	<b>max nat</b>	<b>ens nat</b>
2002	-	-	-	-	-	0.12	0.4	0.27	0.93	0.44
2003	0.03	0.5	0.04	0.15	0.28	0.11	0.13	0.15	0.9	0.32
2004	0.21	0.17	0.21	0.32	0.22	0.11	0.125	0.14	0.92	0.32
2005	0.13	0.135	0.11	0.27	0.14	0.1	0.08	0.14	0.81	0.31
2006	0.02	0.14	0.17	0.26	0.12	0.02	0.04	0.03	0.17	0.08
2007	0.22	0.15	0.18	0.27	0.22	0.02	0.03	0.03	0.83	0.09
2008	0.24	0.23	0.2	0.37	0.3	0.02	0.03	0.14	0.79	0.21
2009	0.22	0.26	0.21	0.35	0.27	0.02	0.01	0.14	0.81	0.18
2010	0.21	0.25	0.27	0.38	0.3	0.01	0.13	0.24	0.87	0.27
2011	0.21	0.14	0.13	0.34	0.22	0.01	0.11	0.29	0.53	0.28
2012	0.29	0.28	0.29	0.41	0.34	0.05	0.11	0.295	0.53	0.32
2013	0.24	0.27	0.28	0.38	0.3	0.01	0.01	0.29	0.16	0.06
2014	0.23	0.31	0.28	0.42	0.33	0.01	0.04	0.3	0.15	0.06
2015	0.23	0.3	0.28	0.41	0.33	0.01	0.18	0.29	0.15	0.32
2016	0.26	0.3	0.28	0.41	0.34	0.01	0.18	0.3	0.15	0.34
2017	0.26	0.3	0.28	0.42	0.34	0.01	0.19	0.3	0.53	0.29
2018	0.07	0.22	0.1	0.29	0.11	0.05	0.21	0.25	0.53	0.3
2019	0.1	0.24	0.13	0.29	0.15	0.05	0.19	0.25	0.53	0.29
2020	0.12	0.24	0.14	0.32	0.245	0.06	0.17	0.28	0.52	0.3
2021	0.16	0.27	0.31	0.44	0.31	0.06	0.17	0.28	0.53	0.3
2022	-	-	-	-	-	0.06	0.17	0.3	0.53	0.3

## D Model response curves

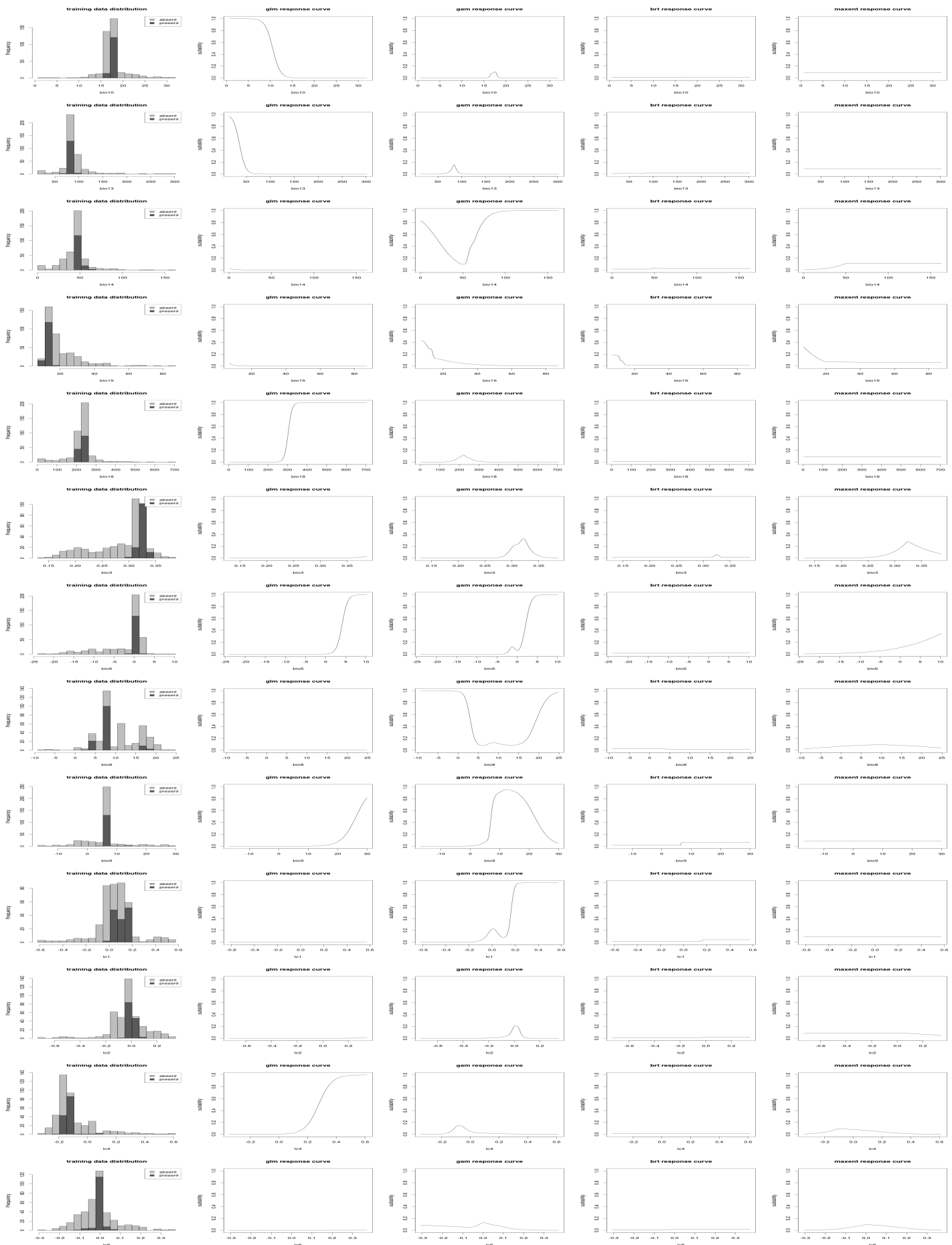
## Native model response curves



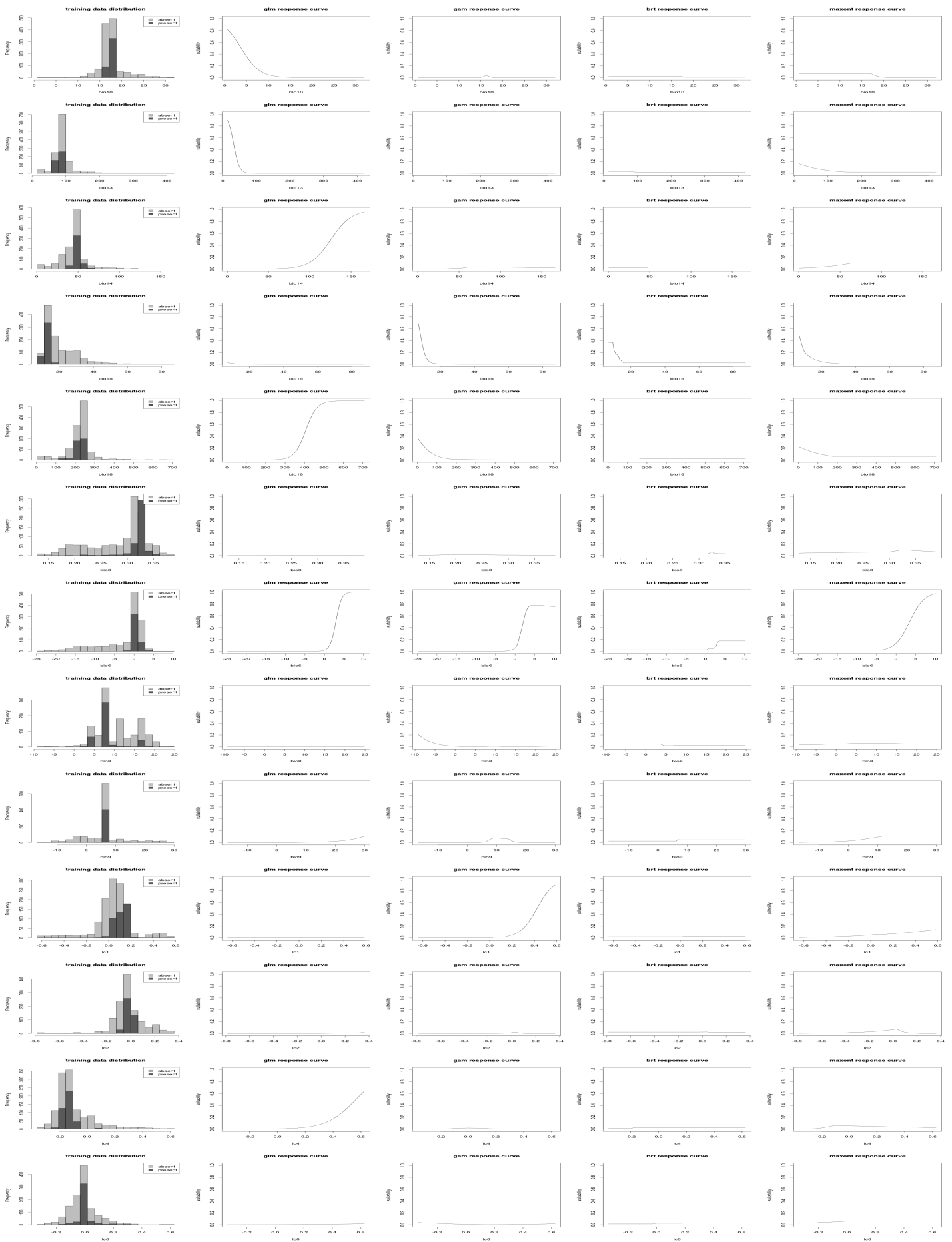
## 2002 model response curves



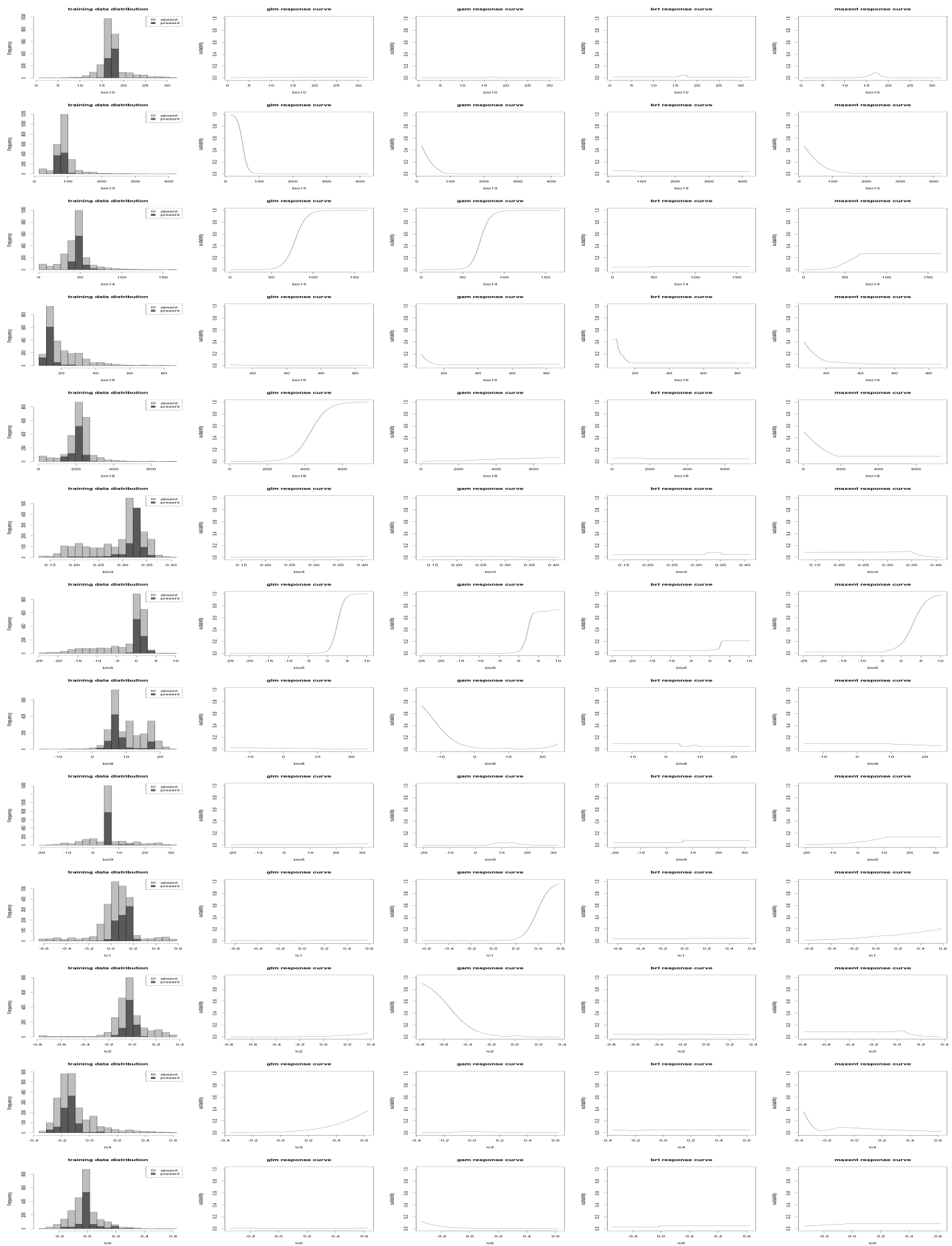
## 2003 model response curves



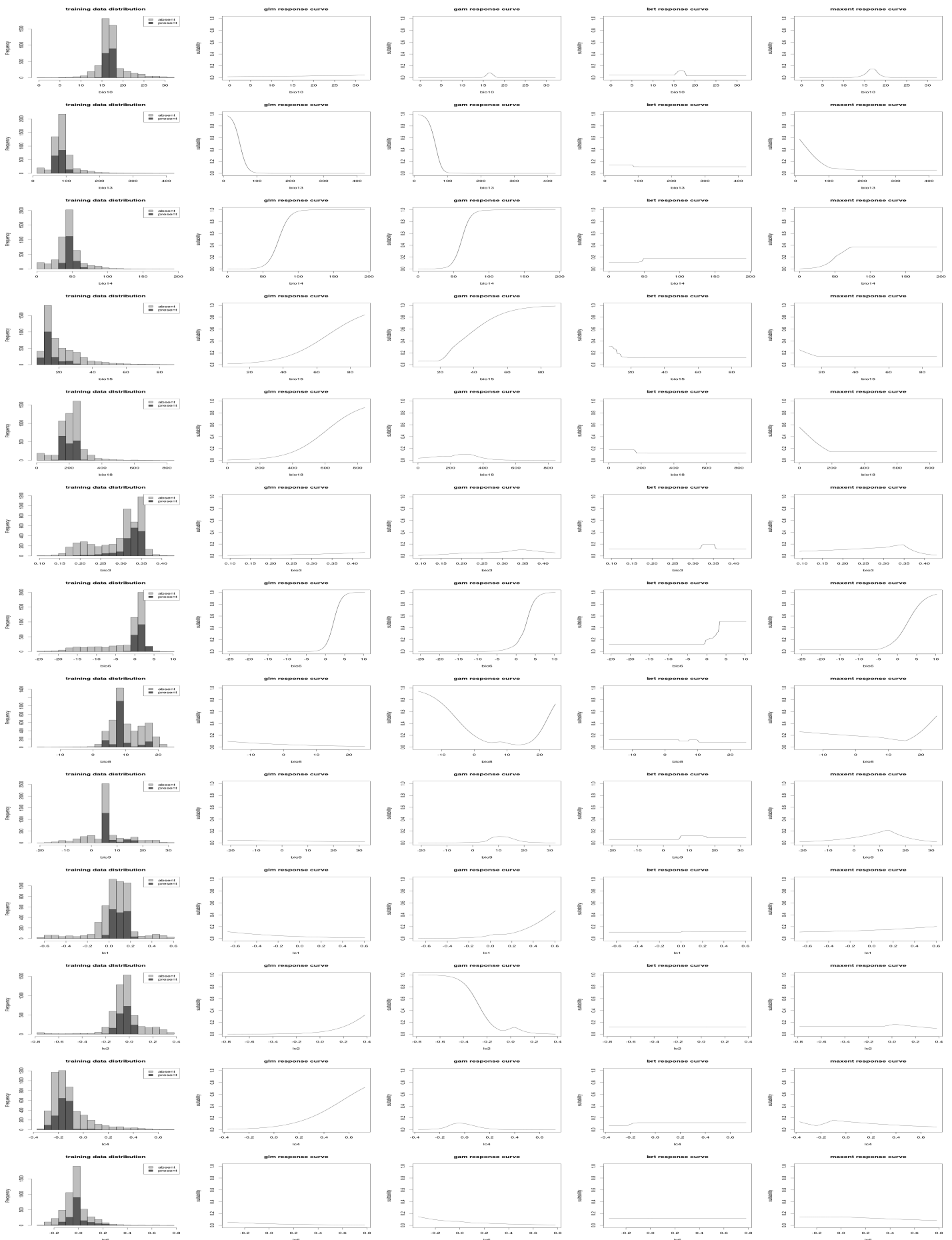
## 2004 model response curves



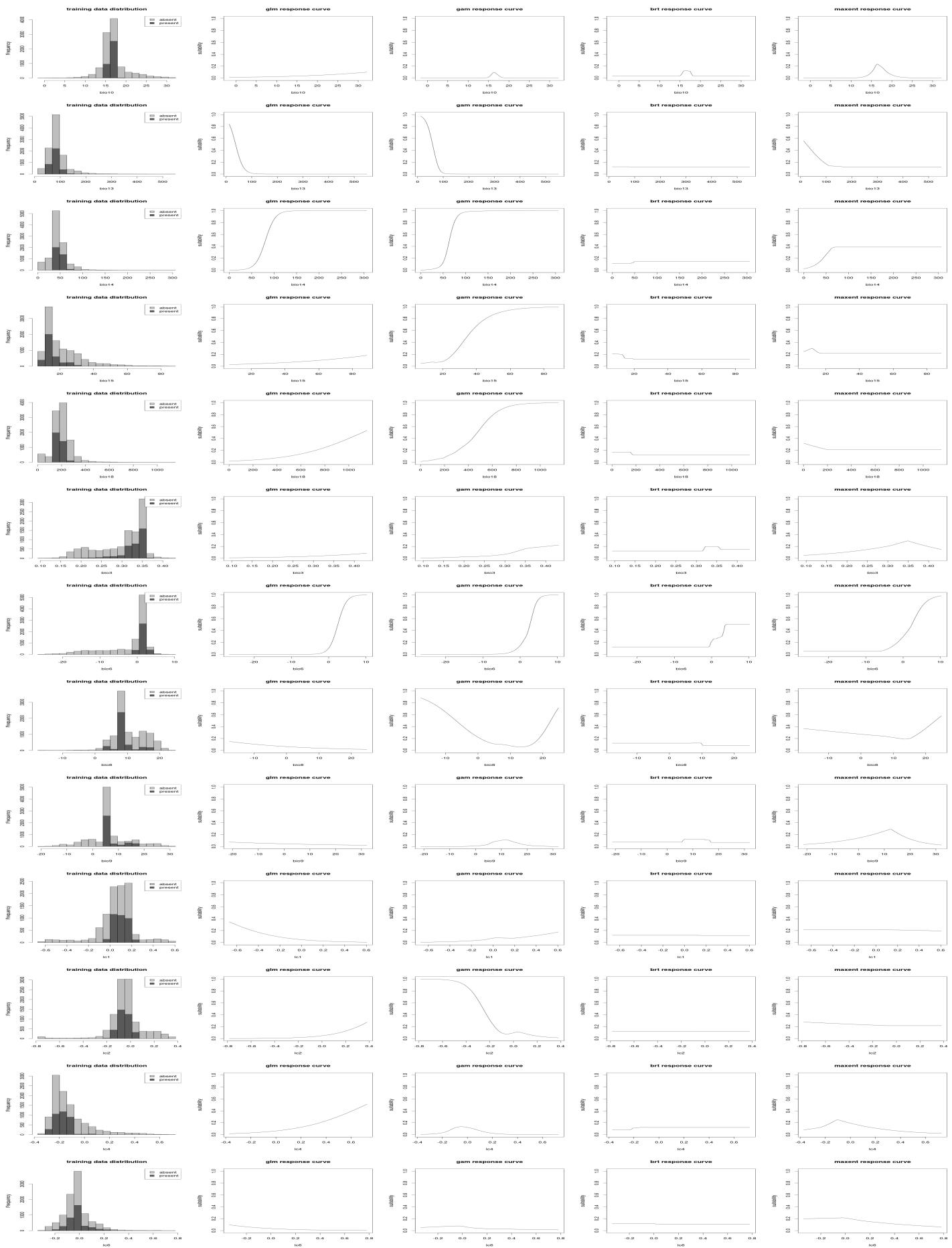
## 2005 model response curves



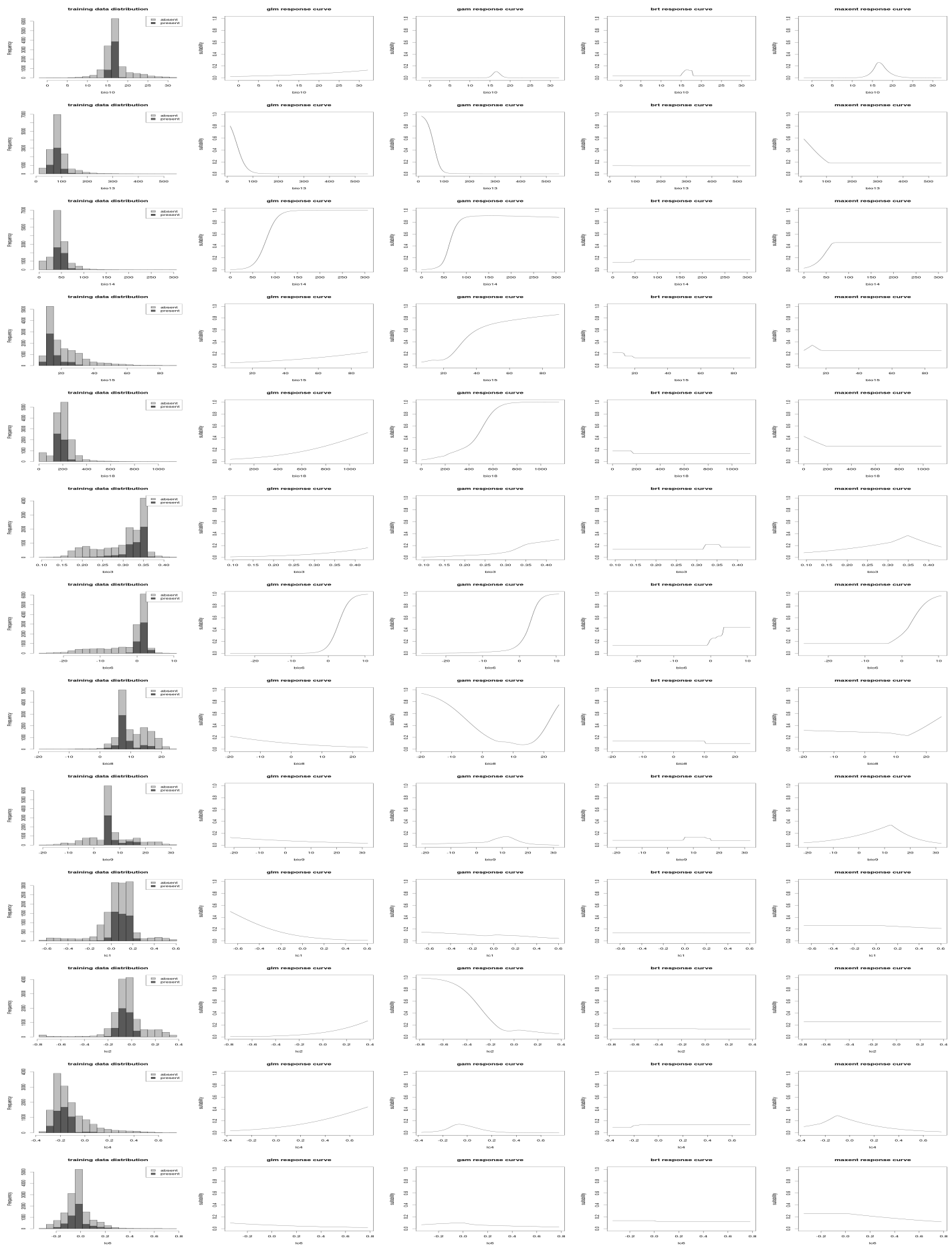
## 2006 model response curves



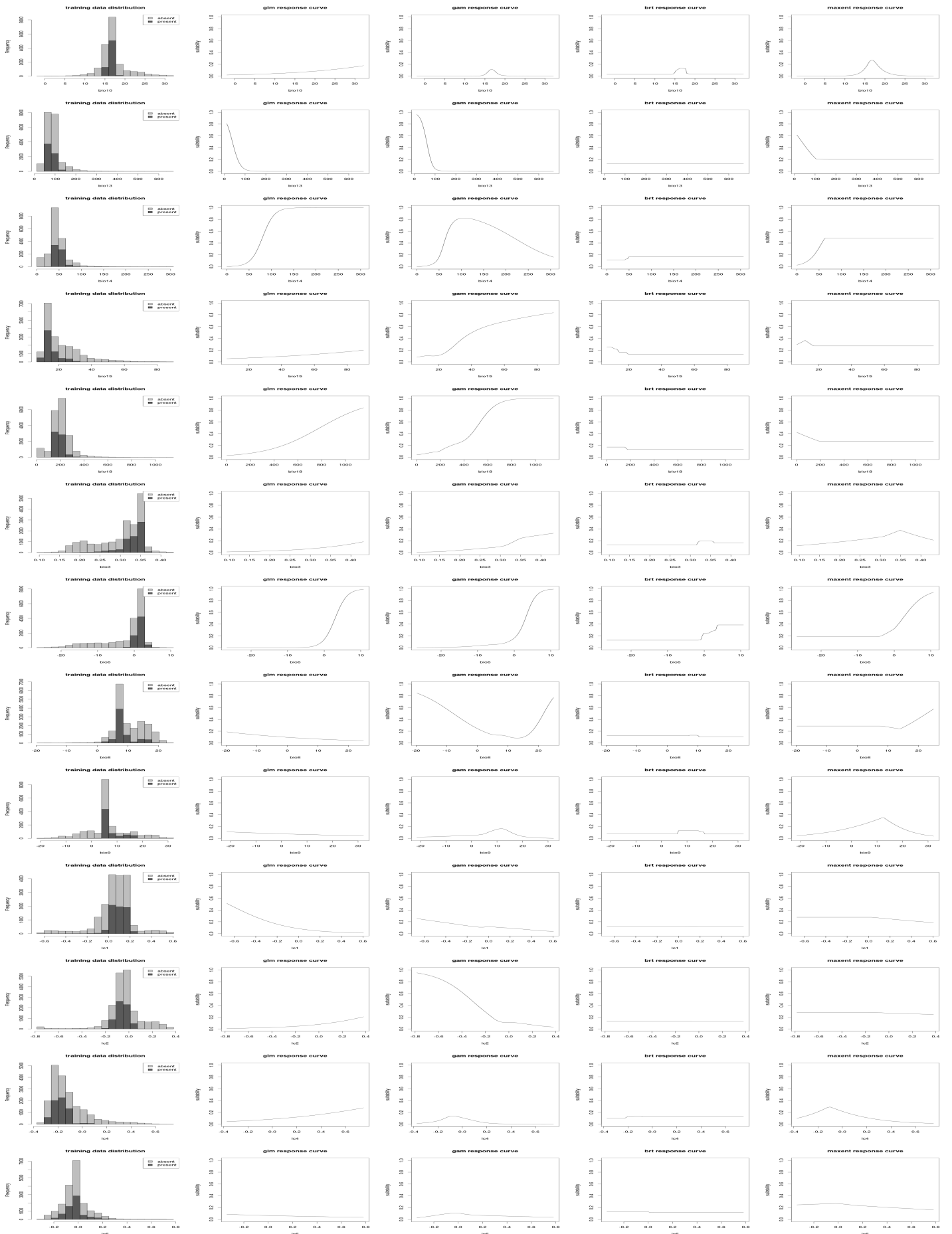
## 2007 model response curves



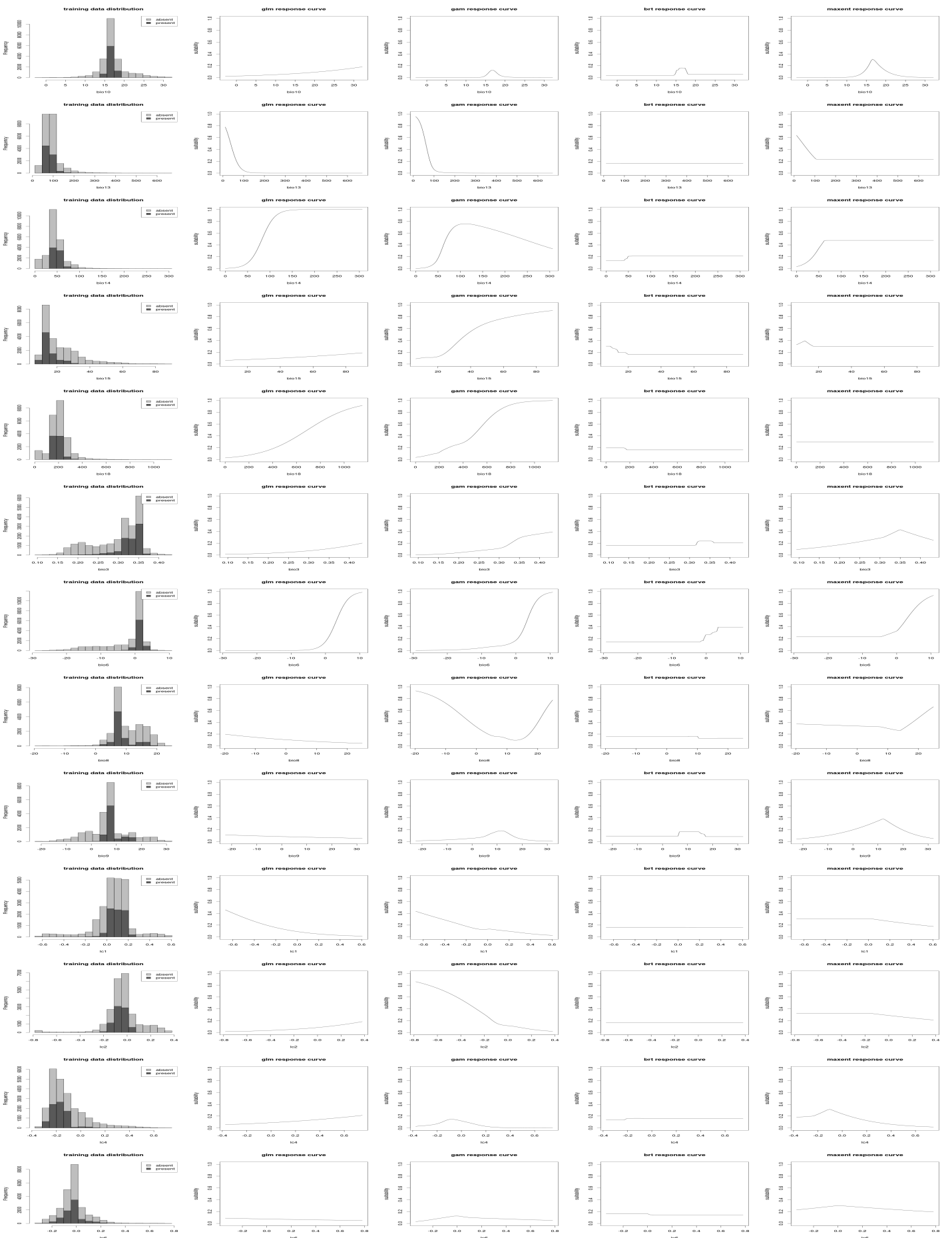
## 2008 model response curves



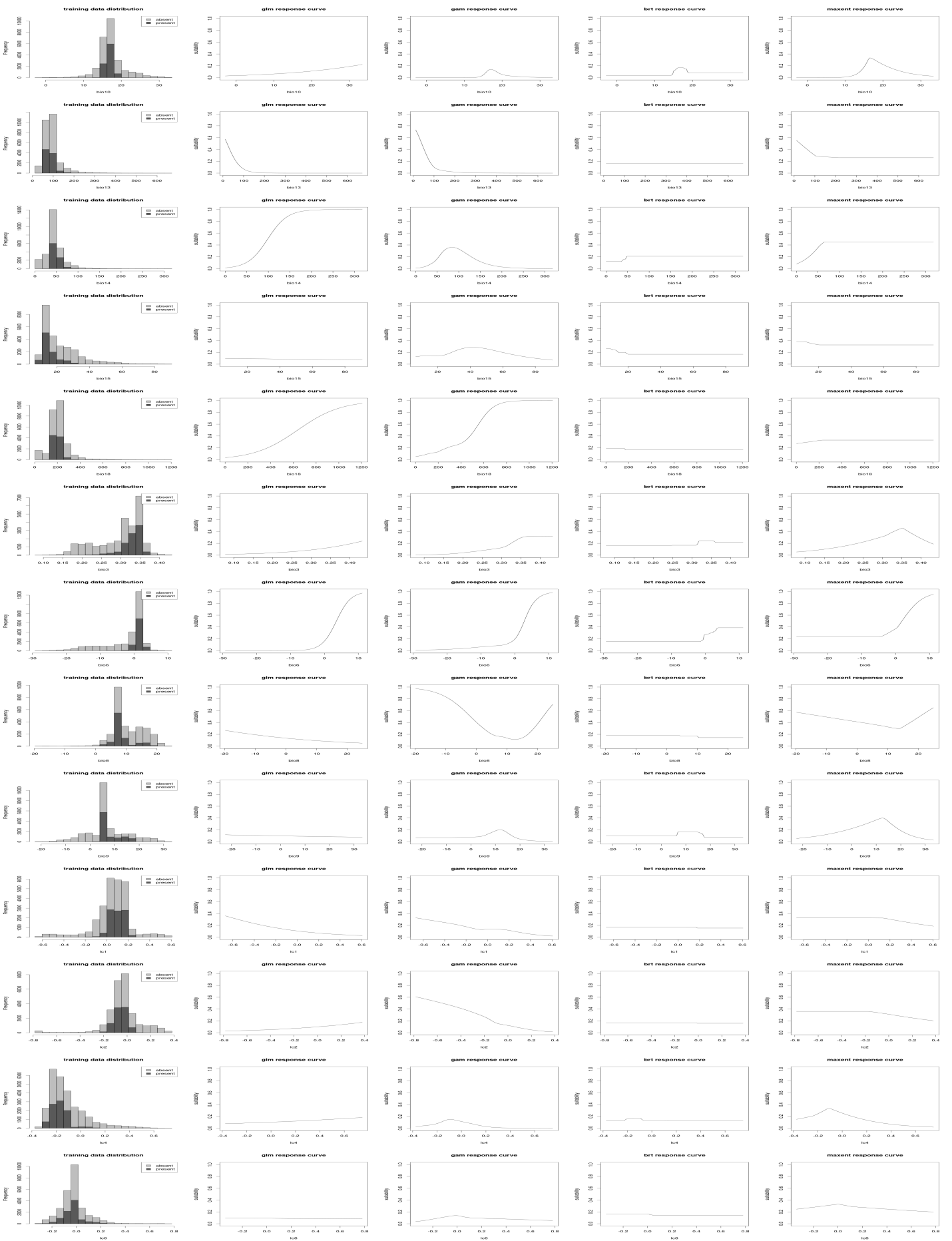
## 2009 model response curves



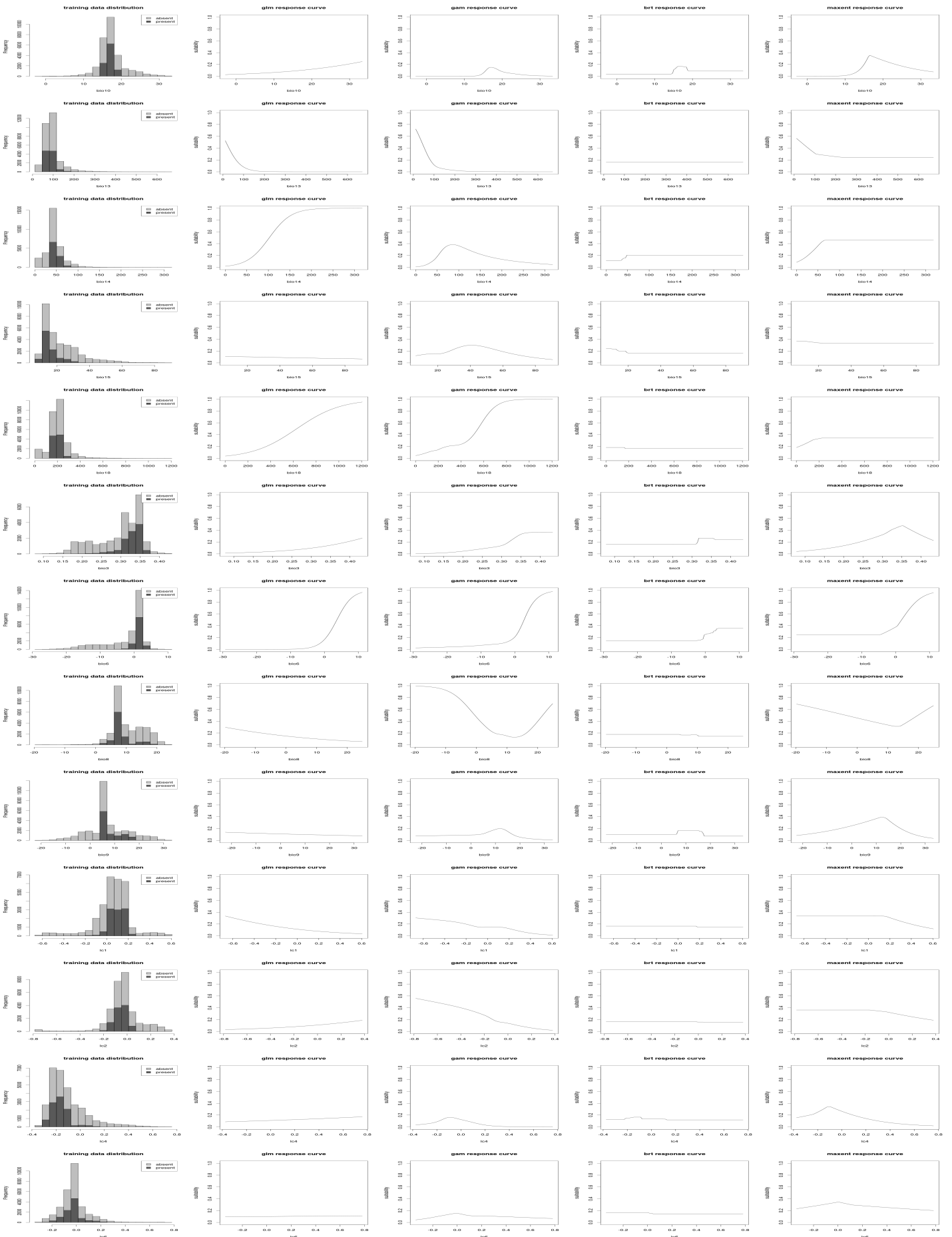
## 2010 model response curves



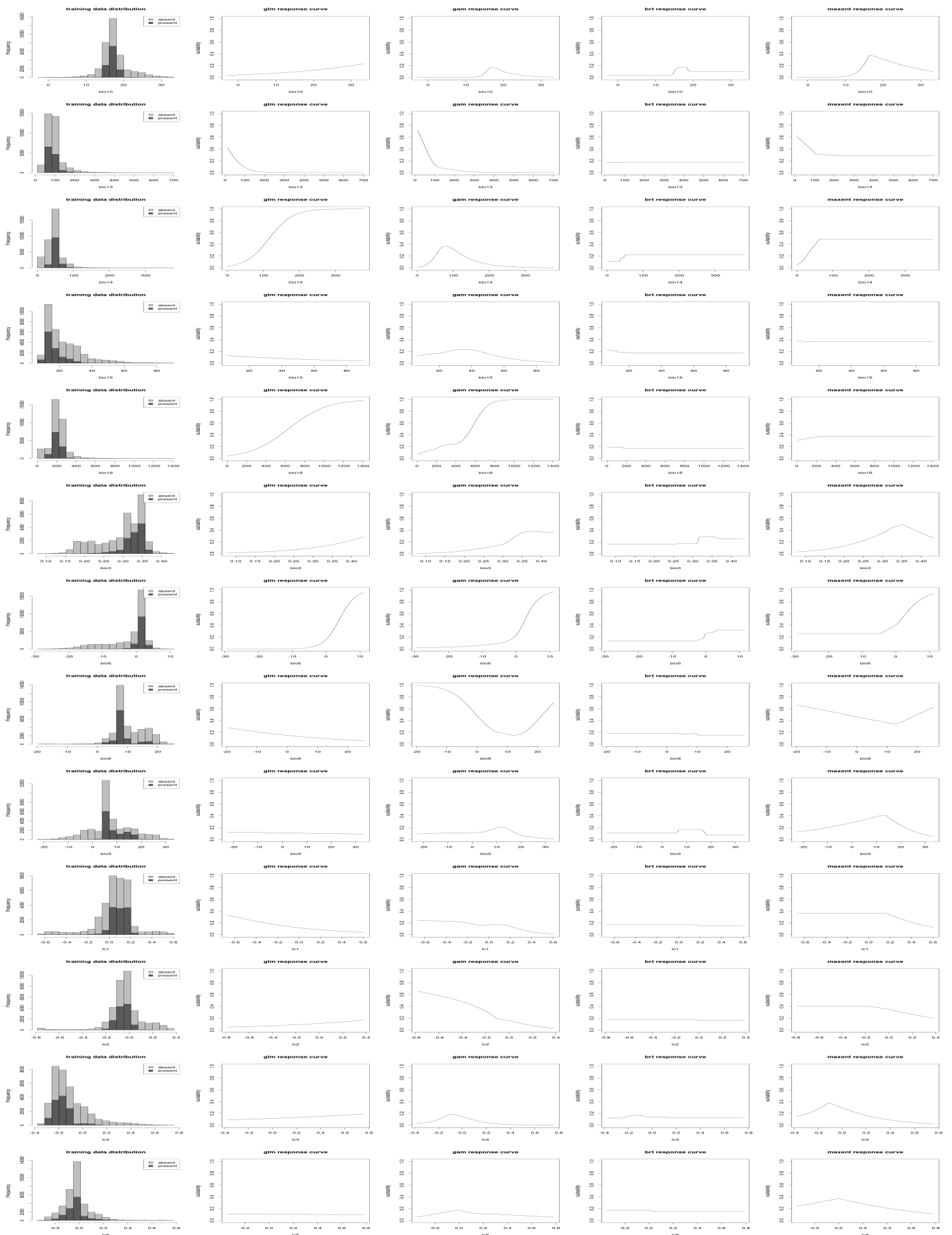
## 2011 model response curves



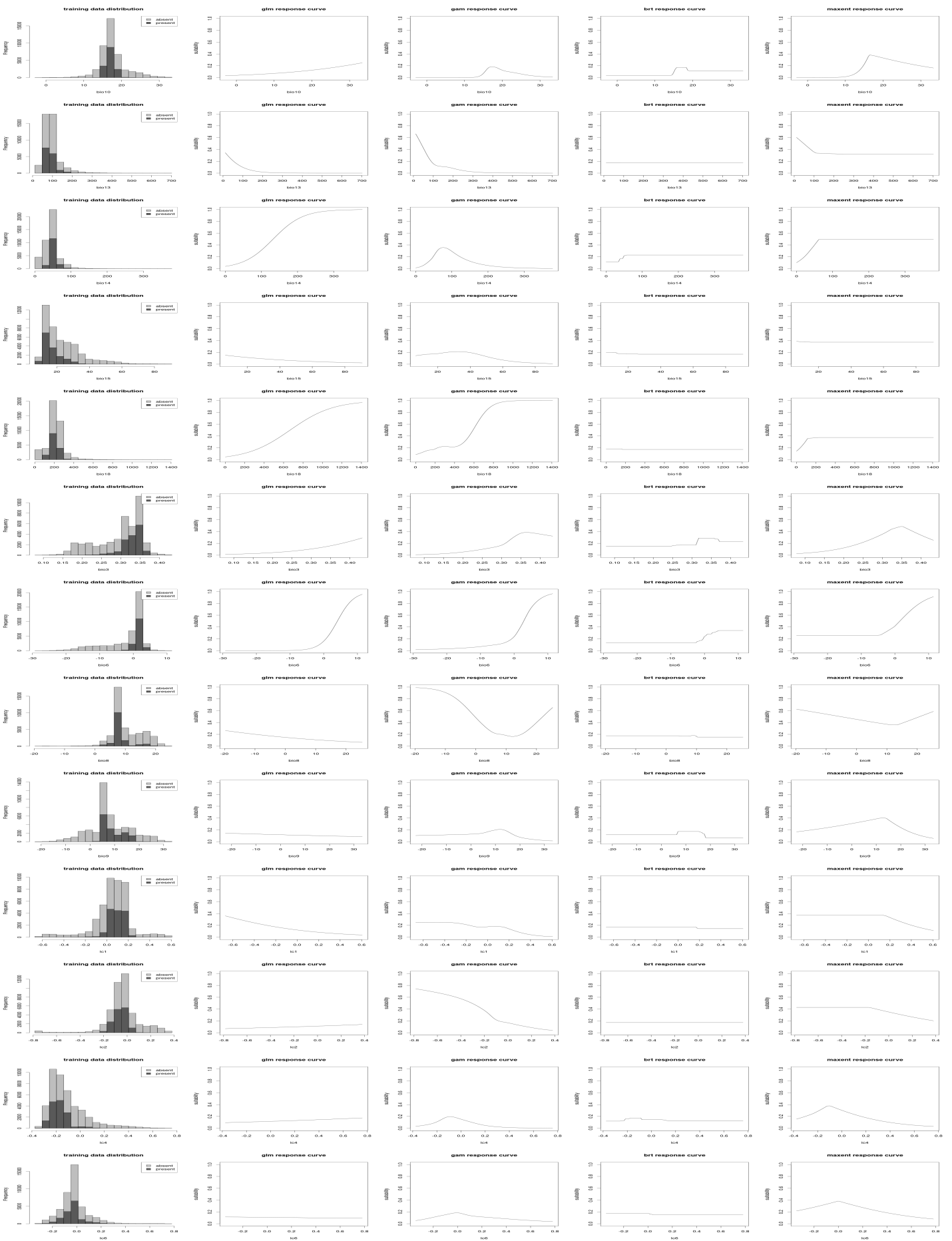
## 2012 model response curves



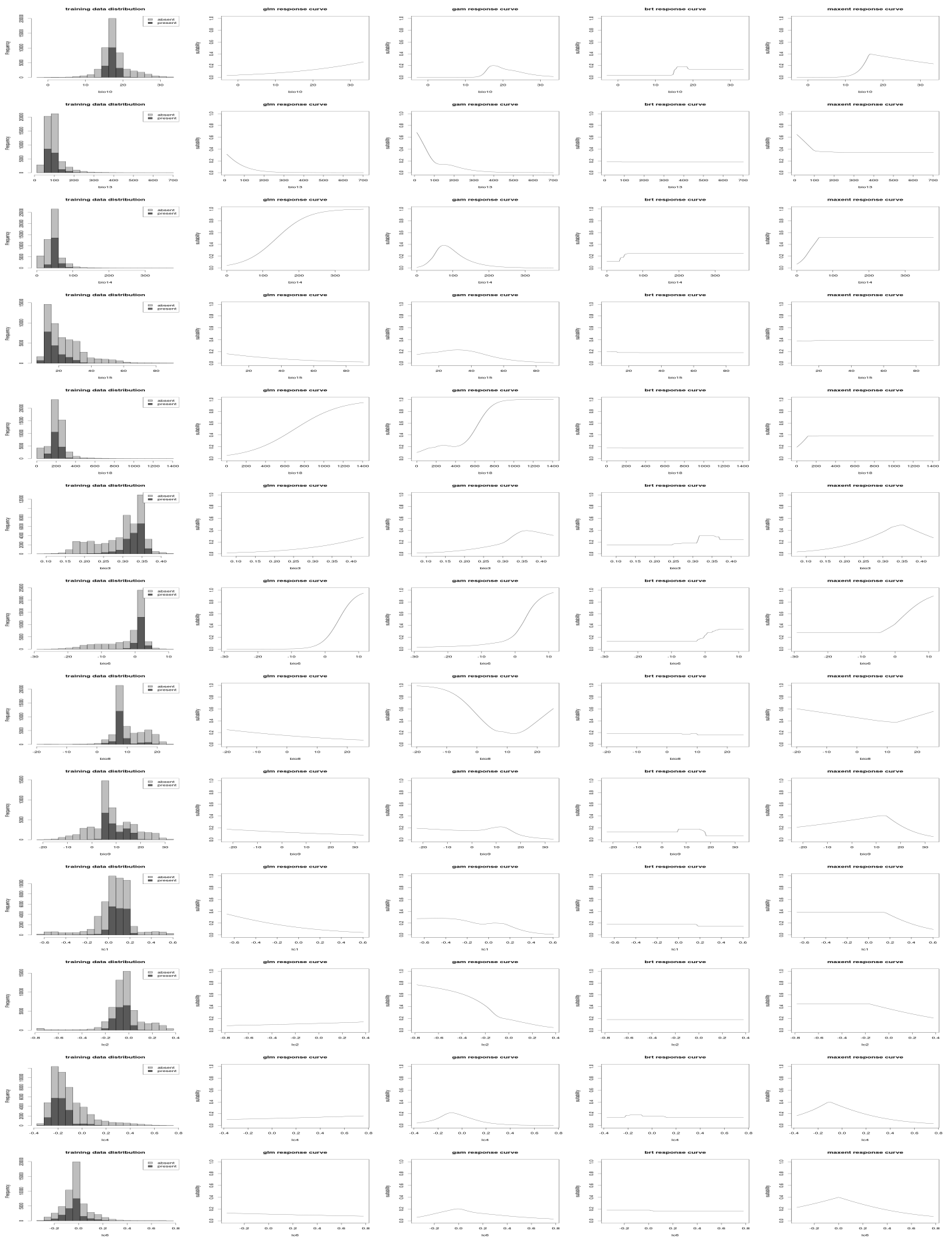
## 2013 model response curves



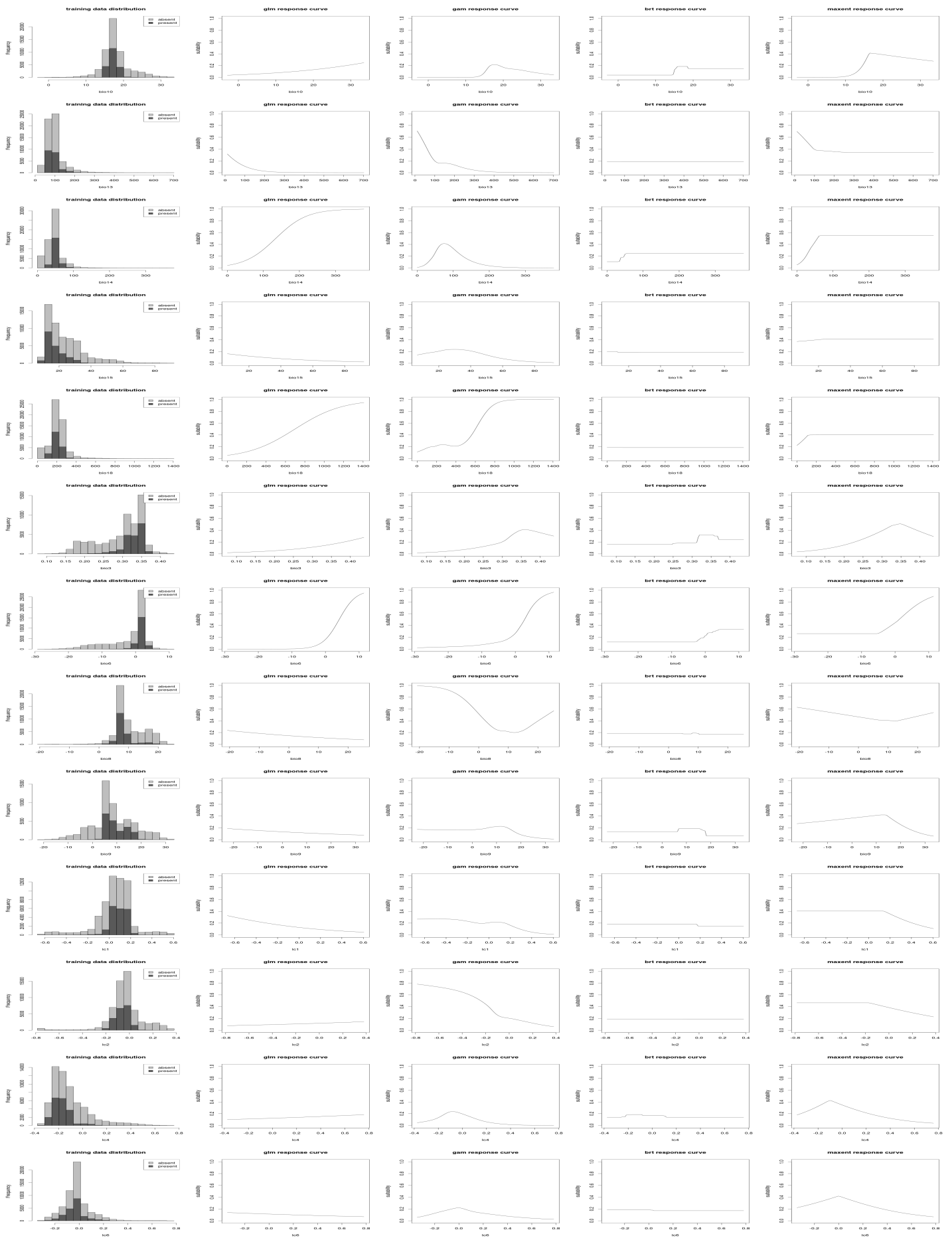
## 2014 model response curves



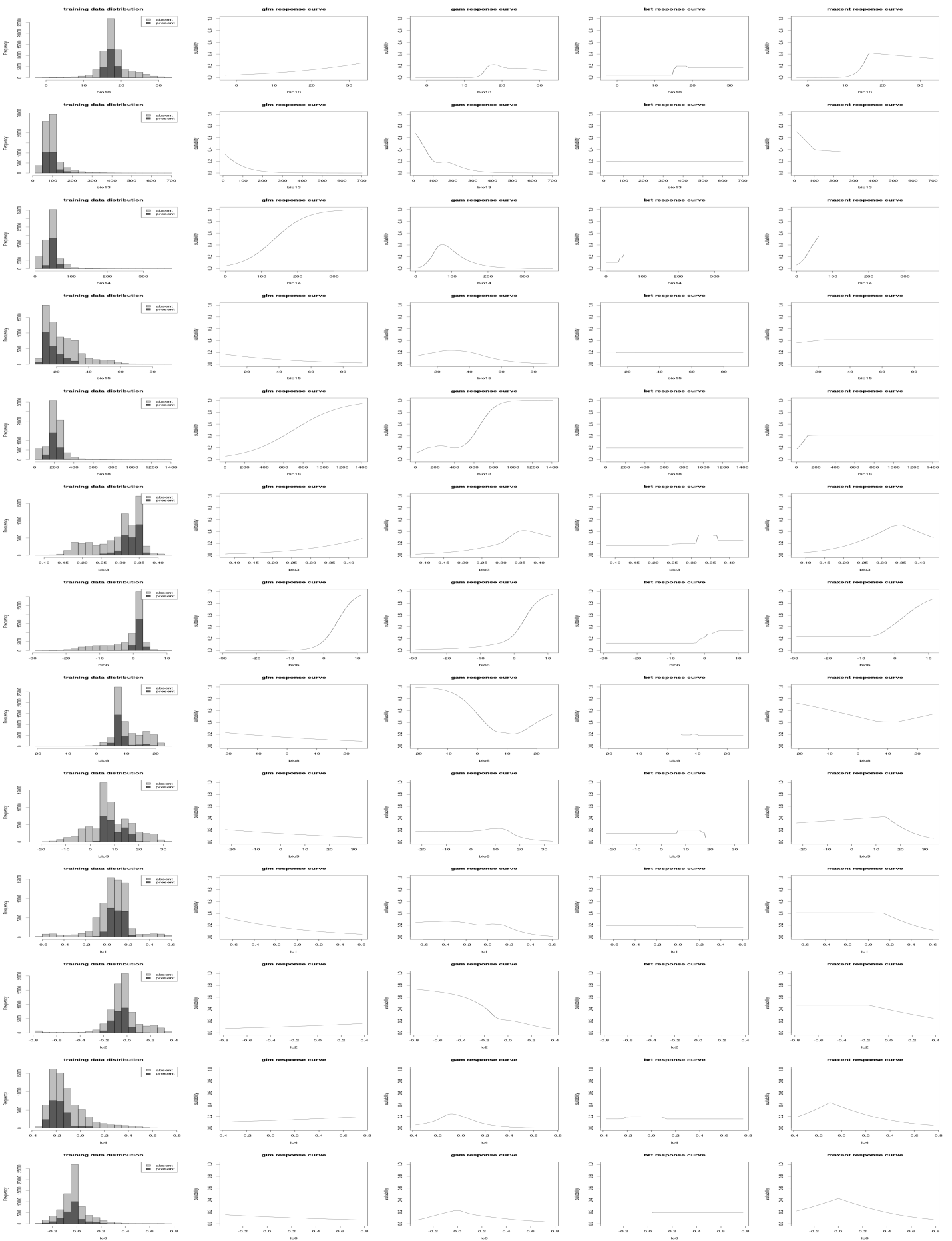
## 2015 model response curves



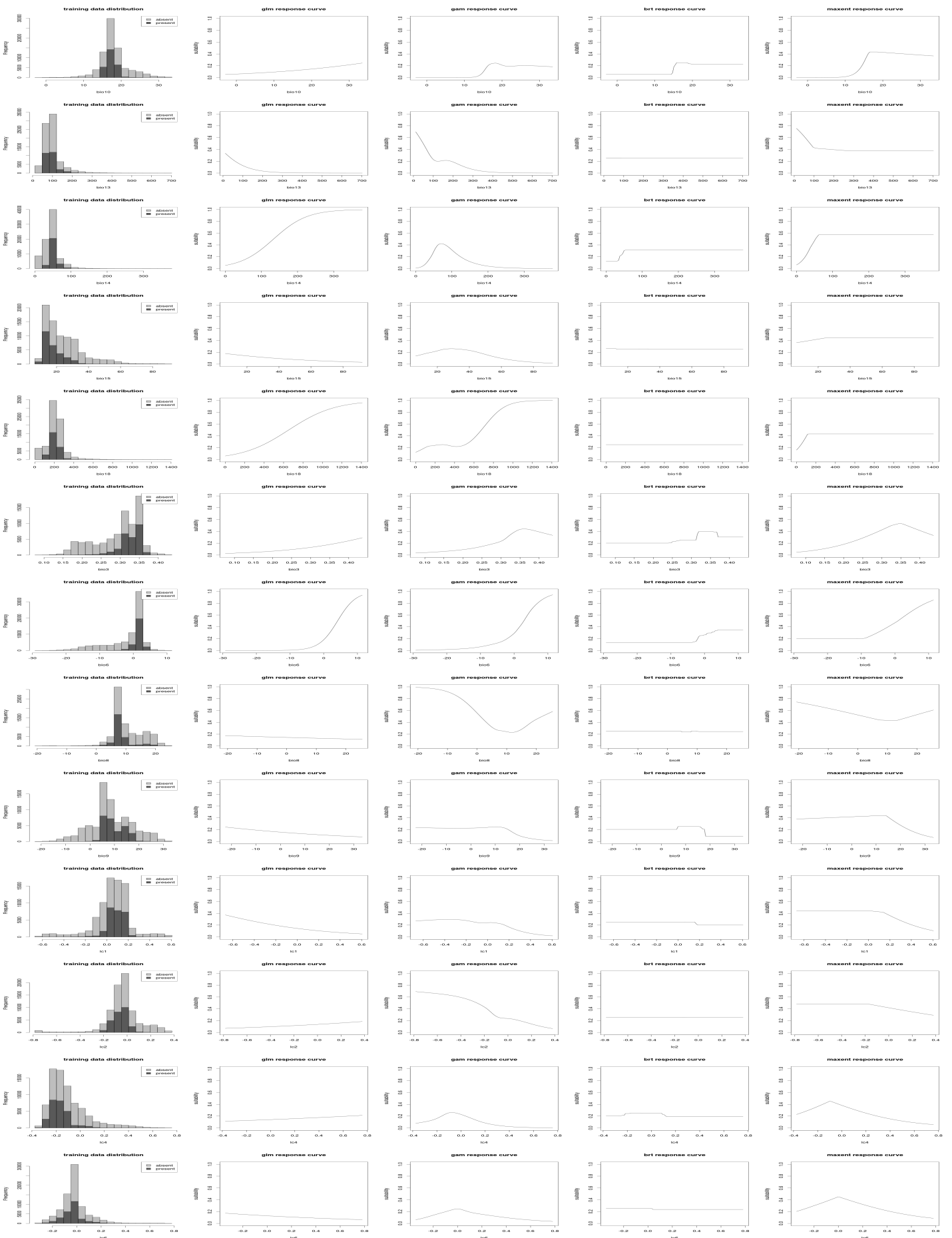
## 2016 model response curves



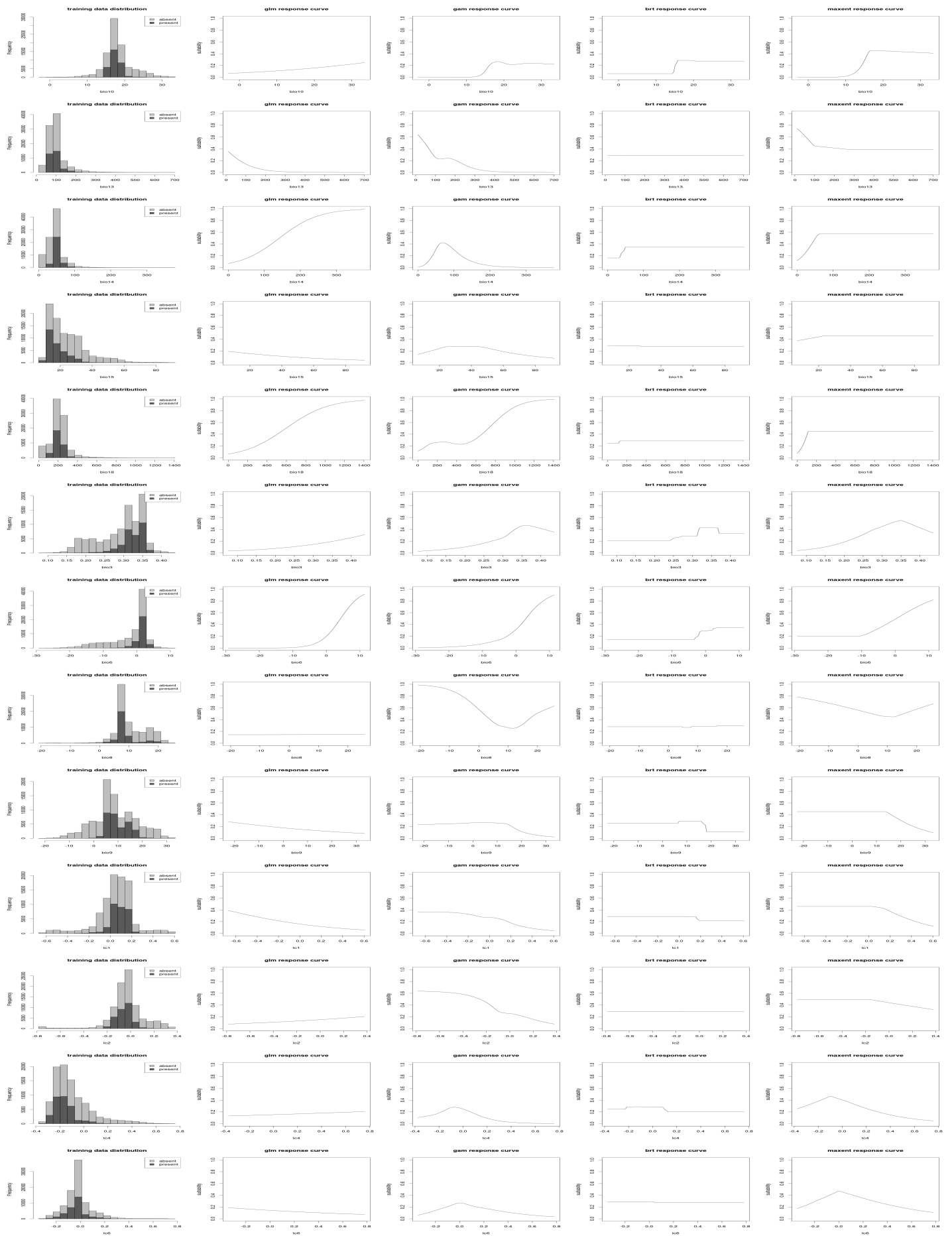
## 2017 model response curves



## 2018 model response curves



## 2019 model response curves



## 2020 model response curves

